CHAPTER 4

Inversion Parameters Testing

The RockMod module in the Jason seismic inversion software was used for geostatistical inversion. After data conditioning, a geostatistical model was constructed by defining a structural framework (solid model) and initial geostatistical parameters (prior PDF and variogram). Simulation parameter testing was then done to generate reasonable geological bodies with respective spatial distribution. Selected sets of parameters, each representing possible scenarios that would honor the seismic data, well log data, and the geostatistical distribution of lithology types in the area were used in the geostatistical inversion. The products of the geostatistical pre-stack inversion were multiple realizations of elastic-properties volumes, consisting of acoustic impedance (AI), Vp/Vs, and density. The inversion also provided lithology volumes in a simultaneous manner. The workflow required careful QC and appropriate selections of parameters in order to provide optimized final results. Due to the limited time available, the inversion parameter testing was performed over a small area (approximately 14 km^2), covering Well-B and –C, where a complete set of geophysical logs was available, including measured shear sonic (Vs) data (see Figure 4.1).

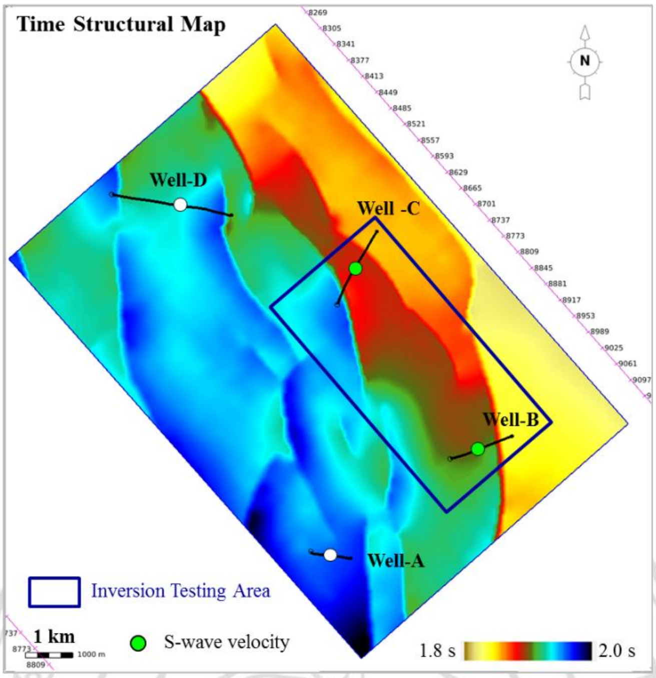

Figure 4.1 Geostatistical inversion testing area (approximately 14 km^2) covering Well-B and Well-C.

4.1 Solid Model Building

After finalizing preparation of the discrete property set (based on well logs), a solid model was constructed. The solid model was constructed by considering similarities of elastic properties and was divided into four layers using five interpreted time horizons (Table 4.1). The solid model used for geostatistical modelling and inversion contained two reservoir layers with high vertical resolution (0.5 ms). Results of the solid model building can be seen in Figure 4.2, illustrated by an arbitrary line passing through all input well locations.

Table 4.1. Stratigraphic layers that were used in the solid model building process.

Layers	Top interface	Sampling Interval (ms)
Top pad	H20	4
Reservoir 1	H30	0.5
Reservoir 2	H37	0.5
Base pad	H44	4

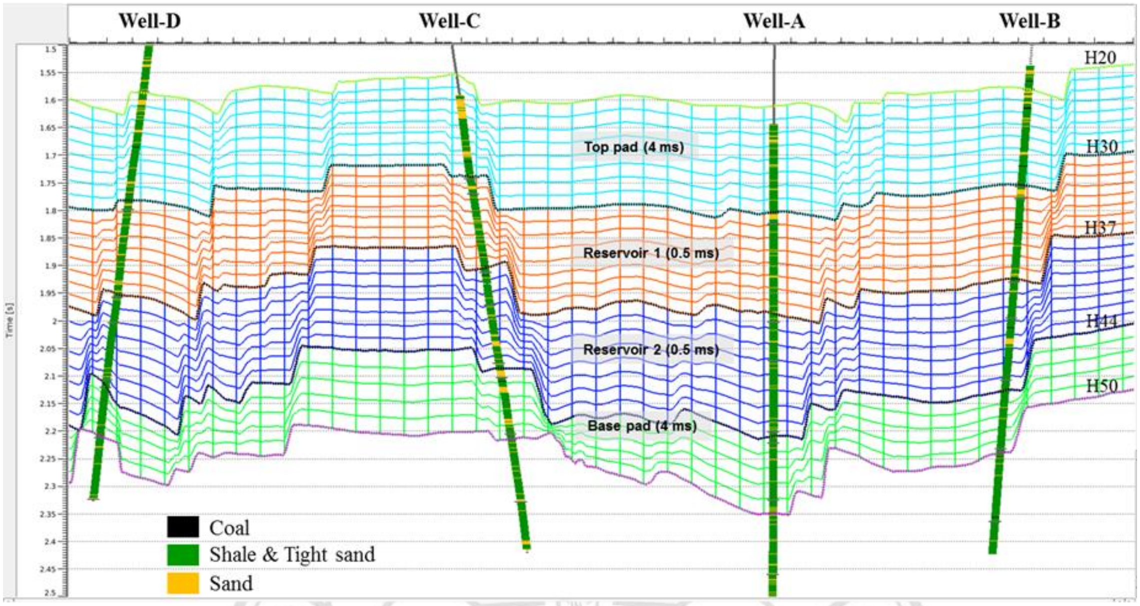

Figure 4.2 The solid model used for geostatistical modelling and inversion.

4.2 Geostatistical Model Fitting

Geostatistical model fitting was carried out to define the prior PDFs and variogram settings for the discrete (lithology types) and continuous properties (elastic properties) models based on well log data.

Probability density functions (PDF) was used to specify the probability of each property. Two types of PDF used in this project: normal and log-normal. Most of the properties were simply fitted by using normal distributions, while some properties such as density and Vp/Vs of shale were best matched using log-normal distributions.

According to elastic property cross-plots, lithology was classified into three groups, namely shale, sand and coal. For discrete property (facies), a 1D PDF or prior proportion of each lithology was derived using well-log data (see Figure 4.3). The prior PDF of the continuous properties (elastic properties) were defined as a joint PDF, and was based on a multi-dimensional probability density function consisting of the PDF of each property and their linear relationships.

In this project, the joint PDFs for both reservoir layers were constructed based on three elastic properties (AI, Vp/Vs, and density) that were obtained from four input wells and resampled to match the resolution of the solid model (0.5 ms). Figures 4.4 and 4.5 show the prior PDF of each continuous property for reservoir layers 1 and 2, respectively.

In general, shale was the dominant lithology type in both reservoir layers with approximately 89%, while sand and coal contributed only 10% and 1% respectively. The data points of shale were sufficient to fit a reasonable PDF, but there was more uncertainty related to the PDF and variogram fitting of sand and coal as there were fewer data points available to describe the optimal elastic property distribution of these lithology types.

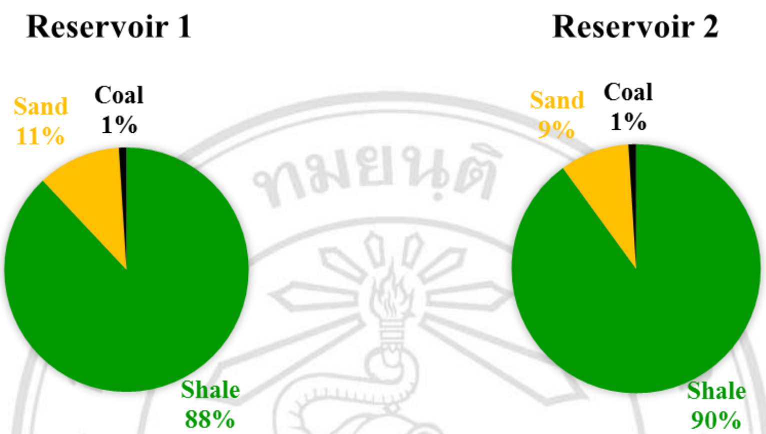

Figure 4.3 1D PDF (prior proportion) for discrete property (facies) in reservoir 1 (H30) and reservoir 2 (H37) layers.

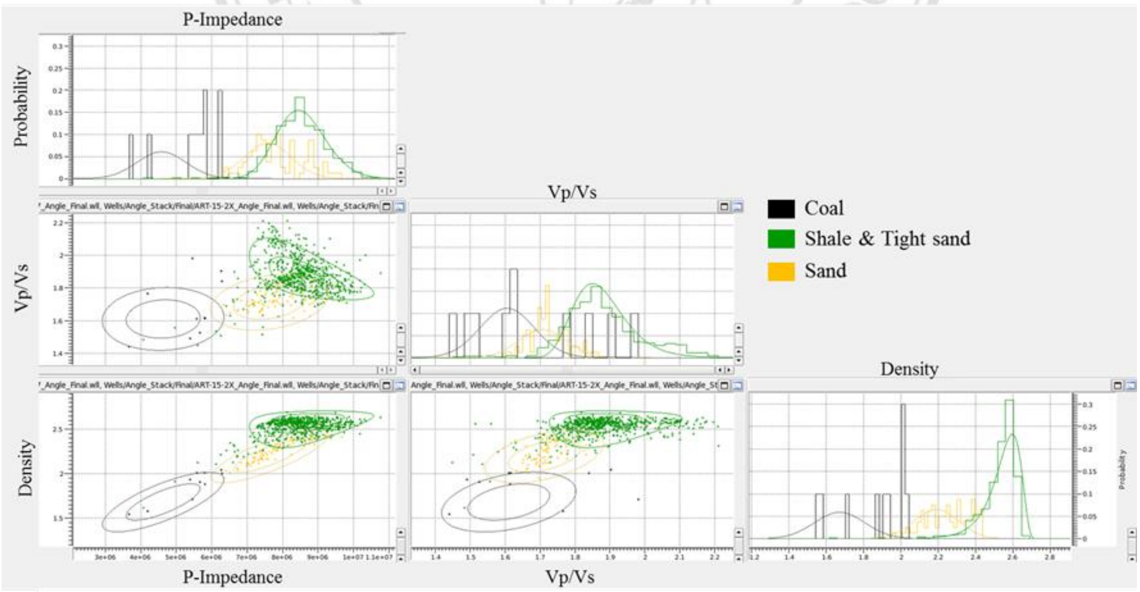

Figure 4.4 A matrix cross-plot showing fitted continuous PDFs of each property in Reservoir 1 (H30). Measured data are represented by points and PDFs are represented by ellipses.

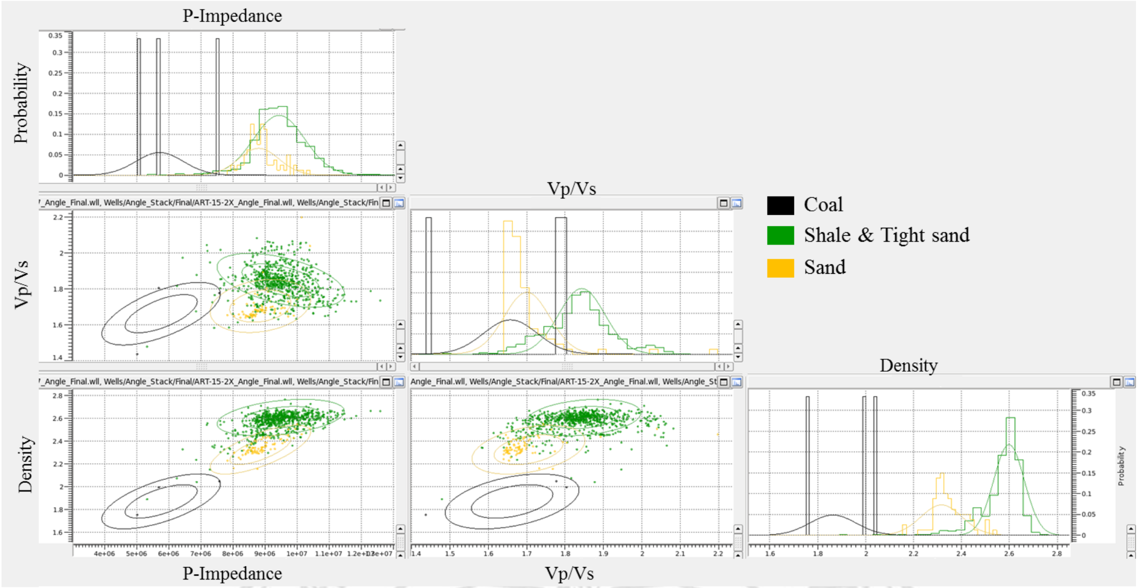

Figure 4.5 A matrix cross-plot showing fitted continuous PDFs of each property in Reservoir 2 (H30). Measured data are represented by points and PDFs are represented by ellipses.

As part of the geostatistical model building, both vertical and lateral variograms of each property were required to control spatial continuity in all dimensions. The vertical variograms were derived from well log data, consisting of lithology, P-impedance, Vp/Vs, and density. Sand probability cubes derived from deterministic inversion results were used to determine lateral variograms. Figures 4.6 to 4.11 demonstrate variogram fitting for discrete and continuous properties for both reservoir layers. Colored points show the experimental variogram calculated from measured data, while solid lines represent the variograms used in the model.

Considering the large number of data samples for shale, fitting of the variogram was carried out with reliable statistics; whereas the statistics of sand contained artifacts due to the sparseness of such data. It is therefore possible that the thin sand reservoirs were slightly statistically biased. However, further adjustments were applied to finalise the geostatistical parameters (PDF and variogram) by performing simulation testing prior to the geostatistical inversion.

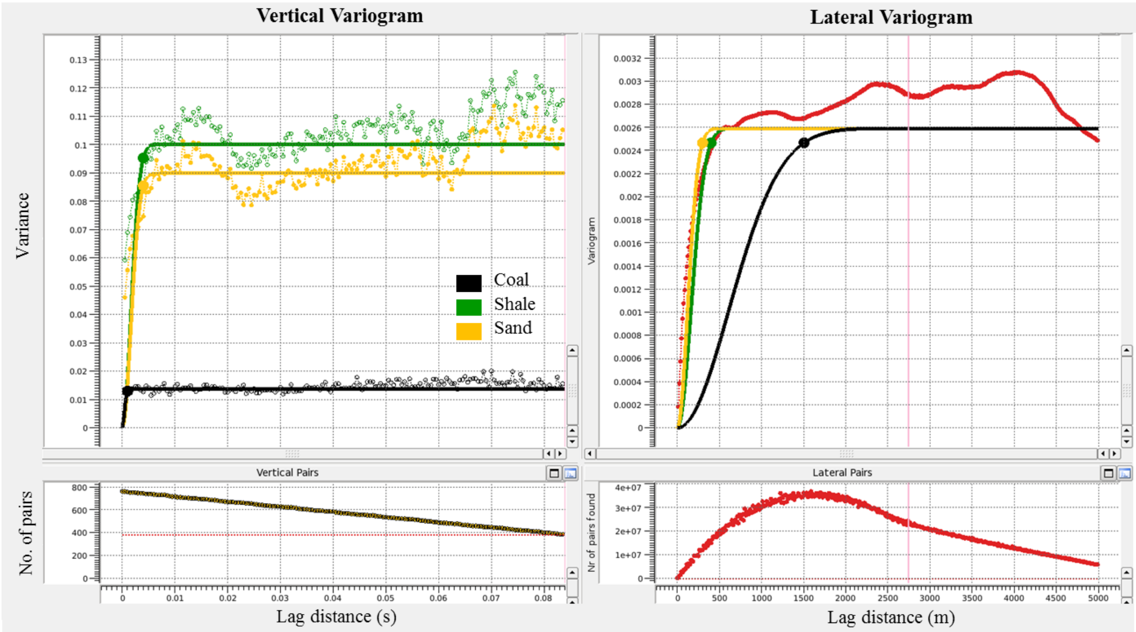

Figure 4.6 Vertical and lateral variogram fitting for discrete properties in Reservoir 1 (H30).

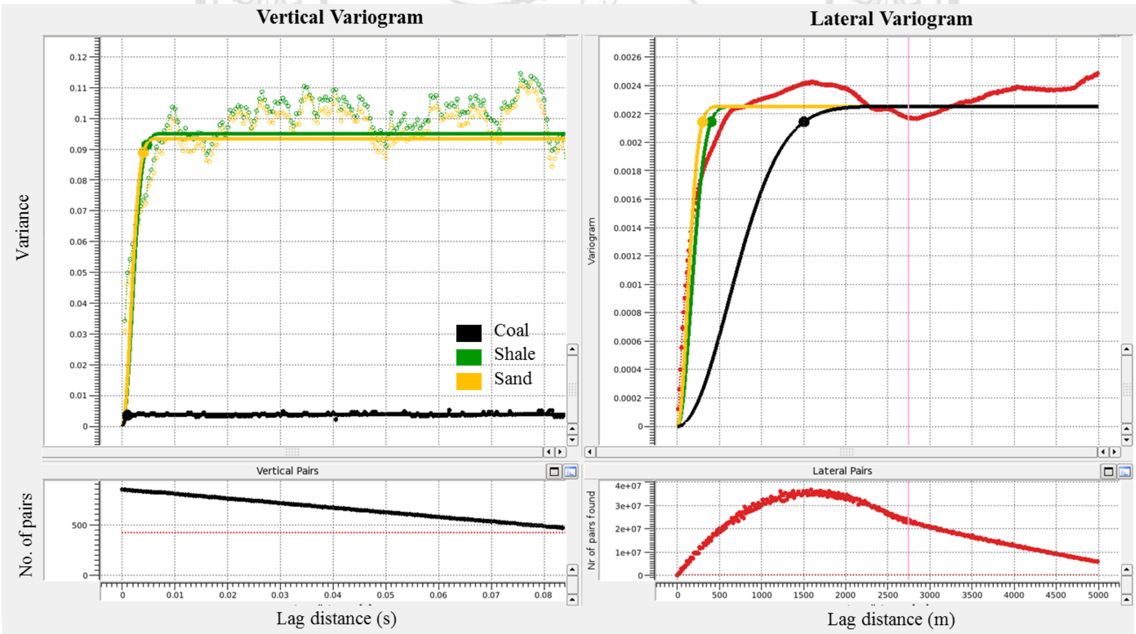

Figure 4.7 Vertical and lateral variogram fitting of discrete properties in Reservoir 2 (H37).

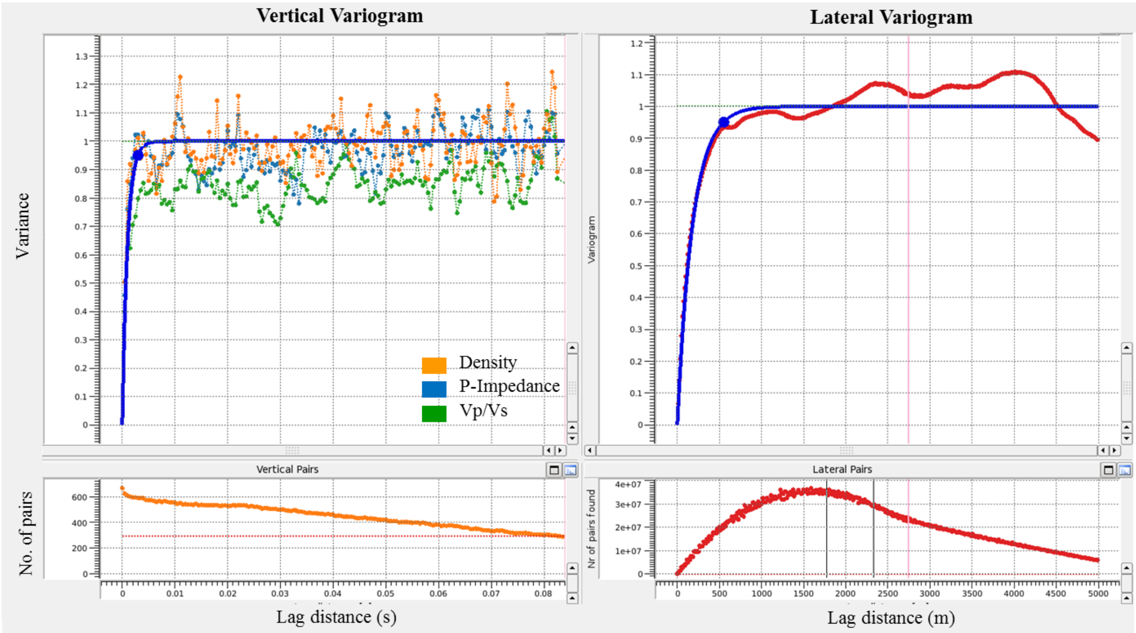

Figure 4.8 Vertical and lateral variogram of shale continuous properties in Reservoir 1.

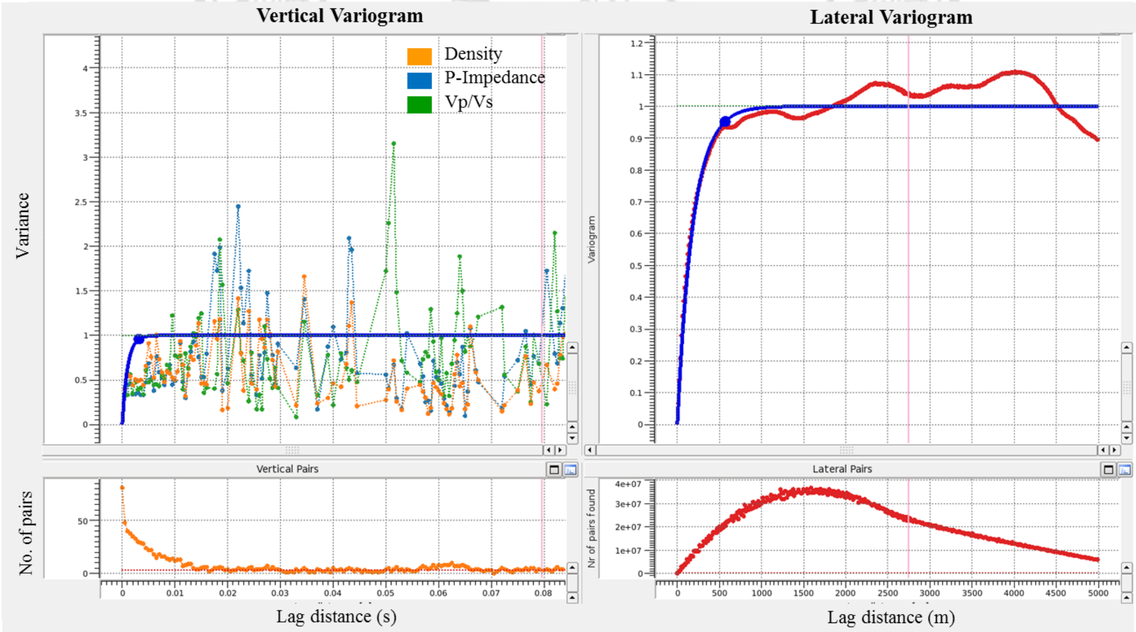

Figure 4.9 Vertical and lateral variogram of sand continuous properties in Reservoir 1.

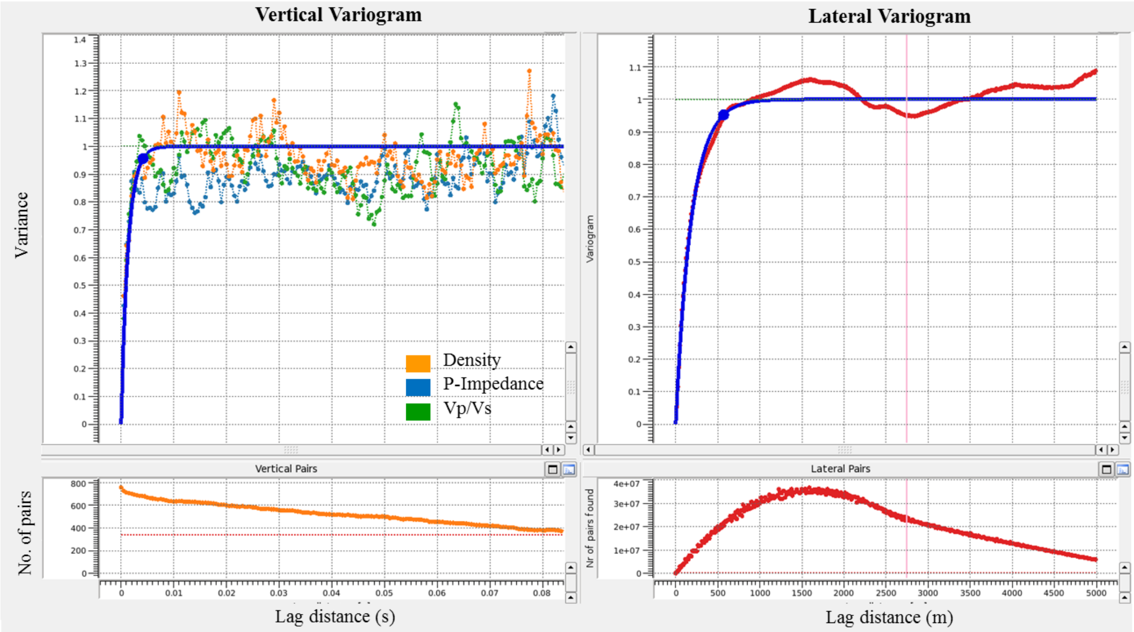

Figure 4.10 Vertical and lateral variogram of shale continuous properties in Reservoir 2.

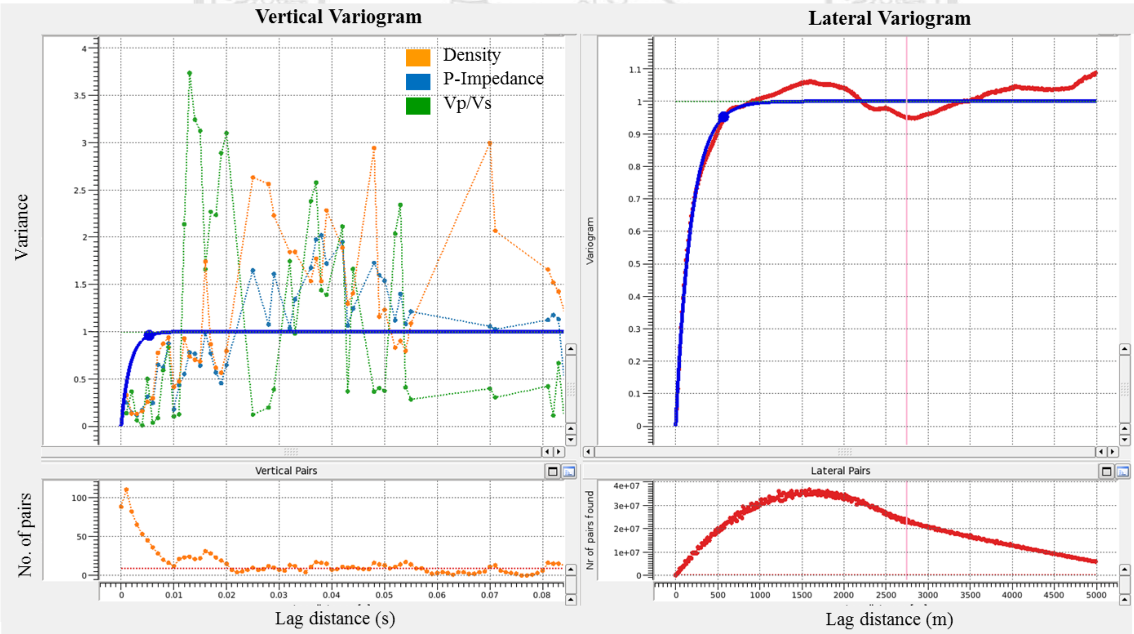

Figure 4.11 Vertical and lateral variogram of sand continuous properties in Reservoir 2.

4.3 Simulation Parameters Testing

Simulation testing was carried out to determine the PDF and variograms for modelling discrete and continuous properties. Several parameter sets were tested for simulation in order to capture the whole range of uncertainty. The results provided a favorite parameter set and also minimum/maximum cases to be used as inputs to the inversion. To capture the range of uncertainty, three simulations were run based on the favourite PDF obtained from the geostatistical model fitting process. The resulting simulation parameters are further described in Table 4.2.

Table 4.2 Simulation settings for discrete and continuous variogram tests.

Simulation Model	**PDF**	**Discrete Variogram**		**Continuous Variogram**	
		Vertical (ms)	Lateral (m)	Vertical (ms)	Lateral (m)
1	Favourite	6	600	6	600
2	Favourite	4	400	4	400
3	Favourite	2	200	2	200

In order to QC simulation parameters, the output statistics from simulation, including posterior proportion and PDFs, should be consistent with prior statistics. Figure 4.12 shows the comparison of prior and posterior proportions (discrete properties) of each lithology type in both reservoirs 1 and 2. The results showed that simulation model 1 overestimated the posterior proportion of sand (prior 7% and posterior 10%), while simulation models 2 and 3 provided reasonable posterior proportions of sand within an acceptable range (prior 7% and posterior 6%).

The comparison between prior and posterior PDFs of elastic properties (continuous properties) generated from simulation models 1, 2 and 3 are shown in Figures 4.13, 4.14, and 4.15, respectively. All simulation models provided similar posterior PDFs that were consistent with the prior PDFs for all lithology types. For each simulation model, a lithofacies section through the wells was generated to observe the lateral distribution of each facies and to compare with the vertical distribution pattern found in well data, as shown in Figures 4.16, 4.17, and 4.18. This analysis showed that the lithofacies section generated from model 1 produced sand bodies that were too thick, too long and overestimated the posterior sand proportion. Both models 2 and 3, however, provided reasonable proportions of sand, but unfortunately model 3 produced sand bodies that were considered to be too thin and discontinuous. Overall the lithofacies section generated from model 2 provided both reasonable proportions and distributions for all lithology types, although it slightly underestimated the posterior sand proportions. Simulation model 2 (medium-range variogram) was therefore determined to represent the favoured parameter set, and was used as input for further inversion parameter testing.

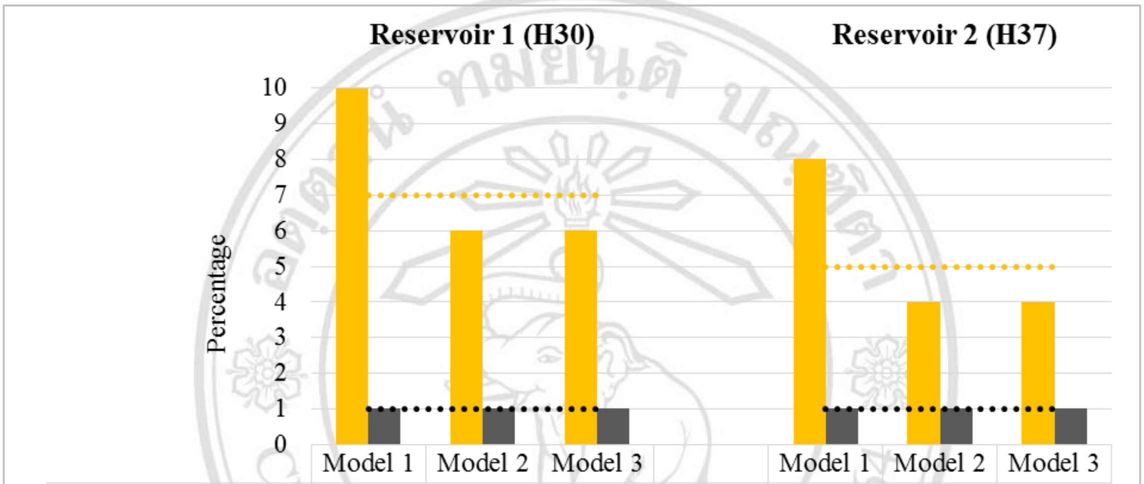

	Reservoir 1 Model 1	Reservoir 1 Model 2	Reservoir 1 Model 3	Reservoir 2 Model 1	Reservoir 2 Model 2	Reservoir 2 Model 3
Posterior (Sand)	10	6	6	8	4	4
Posterior (Coal)	1	1	1	1	1	1
Prior (Sand)	7	7	7	5	5	5
Prior (Coal)	1	1	1	1	1	1

Figure 4.12 Comparison of prior and posterior proportions (1D PDF) of each lithology in reservoir 1 (H30) and reservoir 2 (H37).

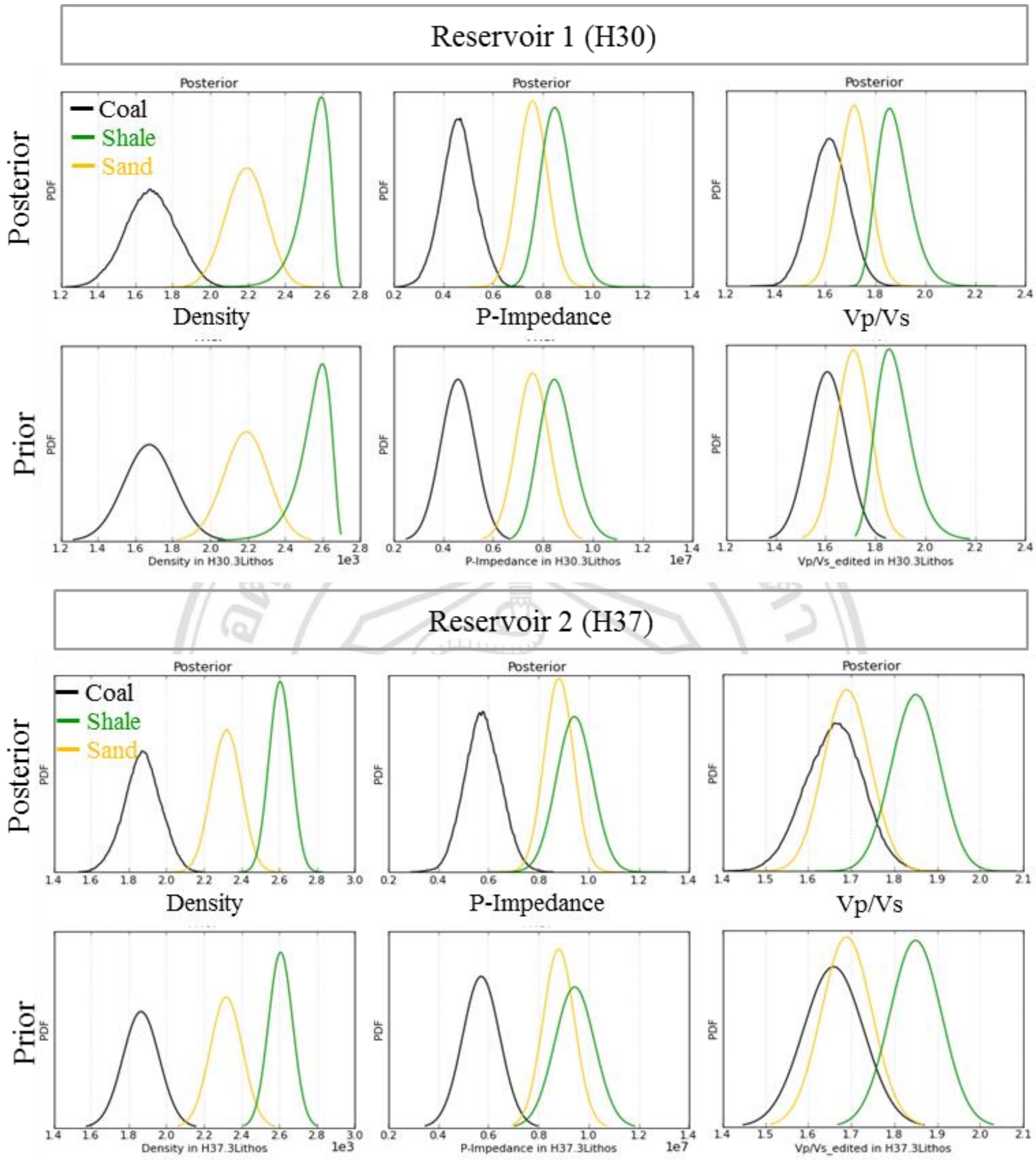

Figure 4.13 Statistical comparison between prior and posterior for all lithologies generated by simulation model 1 (long-range variogram).

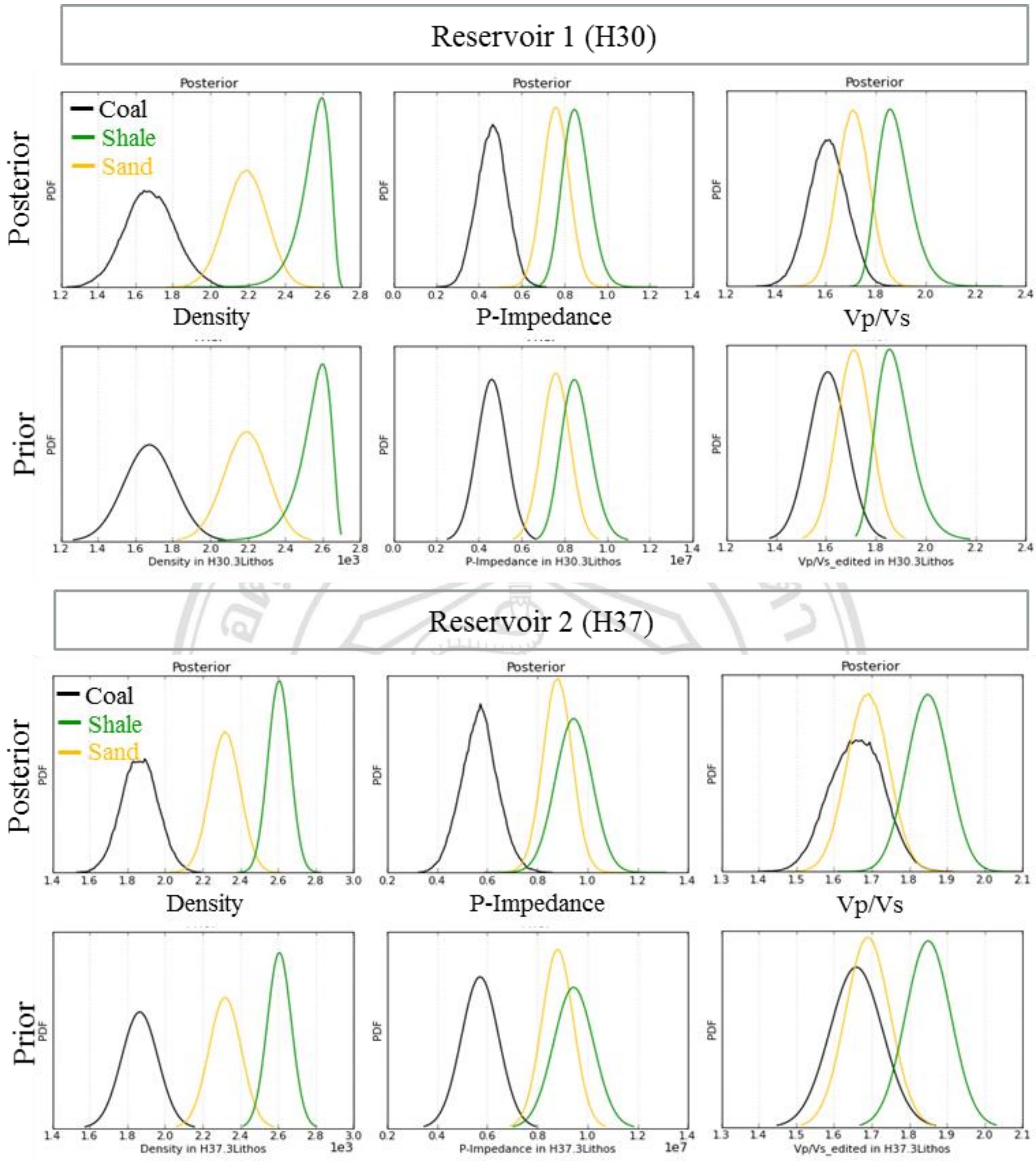

Figure 4.14 Statistical comparison between prior and posterior for all lithologies generated by simulation model 2 (medium-range variogram).

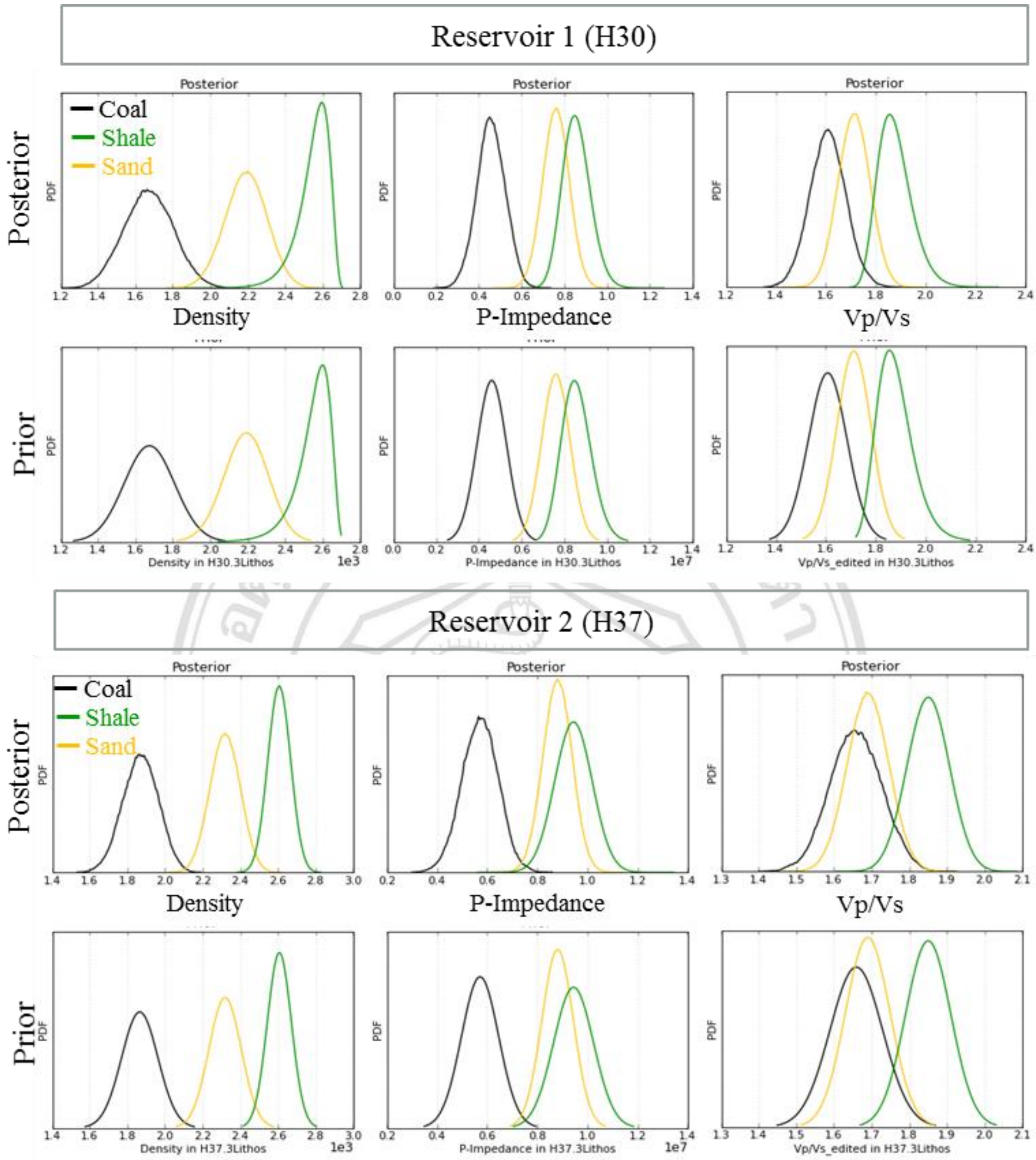

Figure 4.15 Statistical comparison between prior and posterior for all lithologies generated by simulation model 3 (short-range variogram).

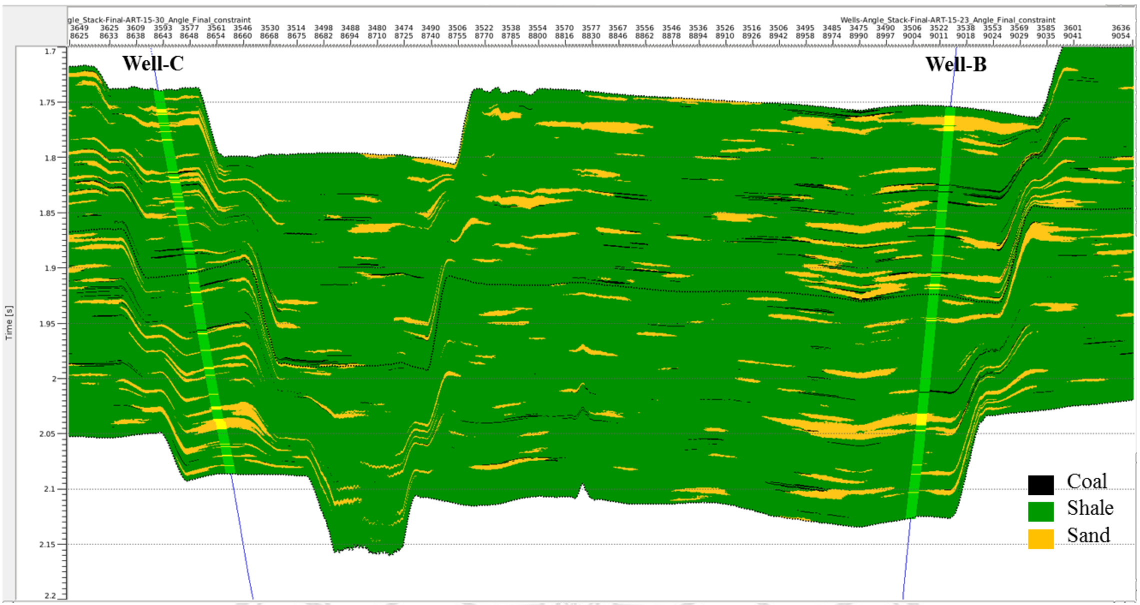

Figure 4.16 Lithofacies section simulated from model 1 (long-range variogram) passing through Well-B and -C.

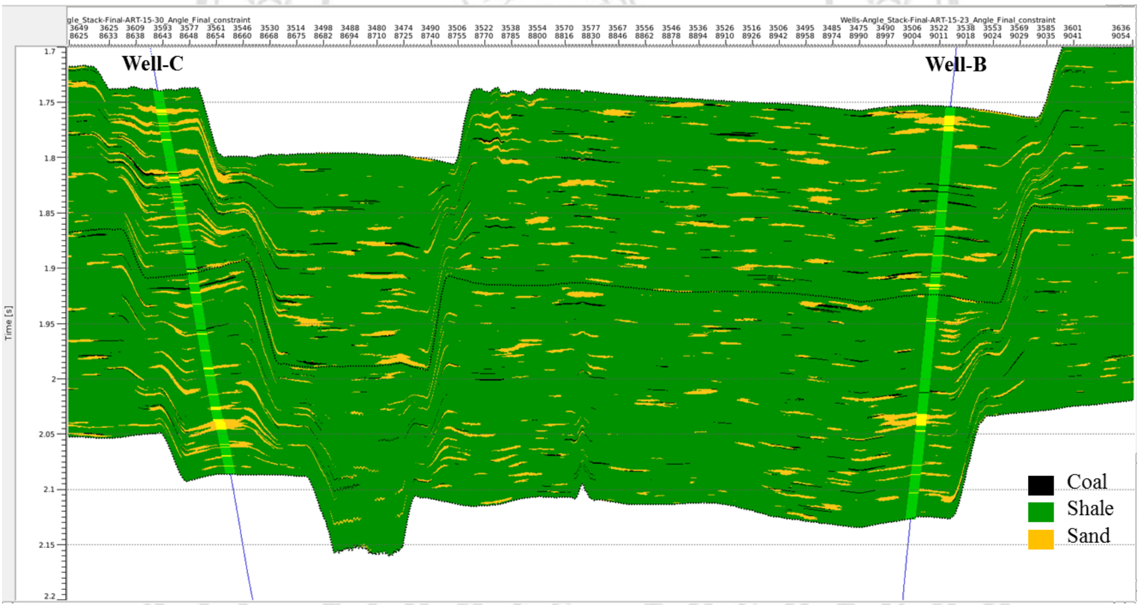

Figure 4.17 Lithofacies section simulated from model 2 (medium-range variogram) passing through Well-B and -C.

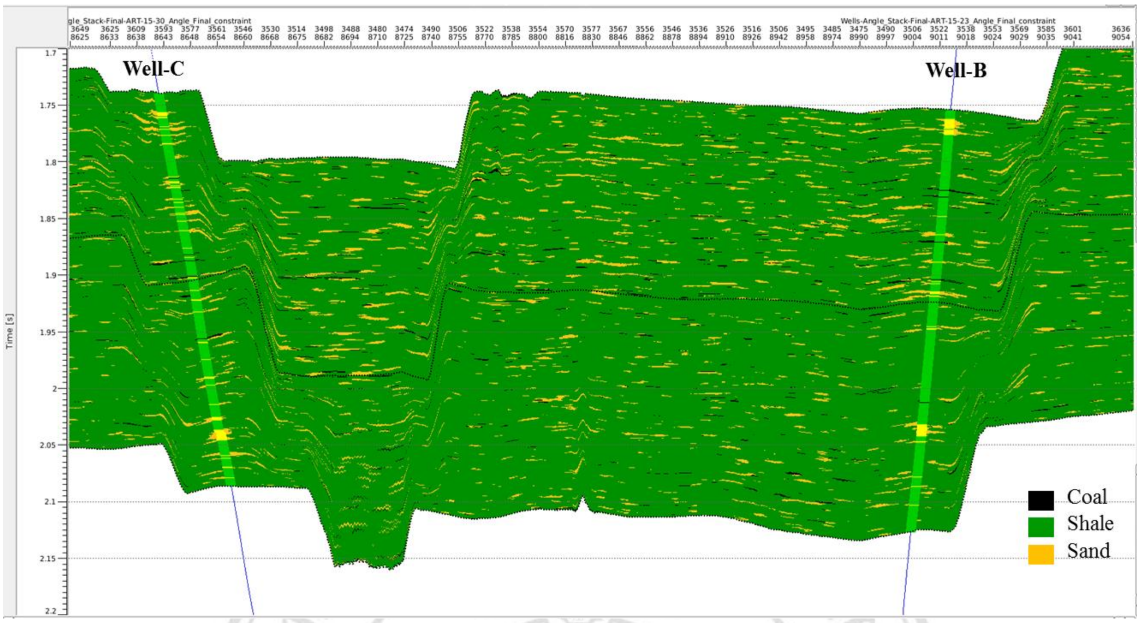

Figure 4.18 Lithofacies section simulated from model 3 (short-range variogram) passing through Well-B and -C.

4.4 Inversion Parameters Testing

In this study, 18 sets of inversion parameters were tested in order to optimize the inversion and capture a reasonable range of the most probable results. All inversion parameter test sets are further described in Table 4.3. Even though the inversion parameter tests included many parameters, it was mainly four parameters that showed significant impact on the inversion results, consisting of variogram range, prior proportion of each lithology, prior PDF, and signal to noise ratio (S/N) of seismic data.

Since eighteen tests produced as many inversion results to evaluate, six examples (Tests 2, 5, 9, 12, 16, 18) were selected to demonstrate the selection and QC process. The QC process involved the comparison of prior and posterior statistics of each lithology type and distribution of each facies compared to the lithologies observed in well-log data.

Conceptually, the posterior proportions constrained by well logs and seismic data through the inversion process should match with input prior proportion derived at wells. As shown in Figures 4.19 and 4.20, Tests 2, 5, and 9 provided extreme overestimation of the posterior sand proportion. By using a short variogram range (Test 5) and decreasing S/N (Test 9) the posterior sand proportion was slightly reduced, but still too high. To resolve this issue, the prior sand proportion was decreased to obtain representative posterior sand proportions (11% for H30 and 9% for H37) in Tests 12, 16, and 18. These tests provided better posterior sand proportion which were closer to the expected sand proportions being derived from input well log data.

Figures 4.21 to 4.26 show lithology and P-impedance sections generated from six inversion tests. As the results show, high prior sand proportions created thick and continuous sand bodies that caused overestimation of the posterior sand proportions in inversion Tests 2, 5 and 9. Therefore, the prior sand proportion was decreased in inversion Tests 12, 16, and 18, which provided reasonable proportions and distributions of sand agreeing with well data.

In addition, the prior PDF of each lithology was adjusted to obtain better posterior PDFs and distributions of each lithology type in inversion Tests 16 and 18. The comparisons between prior and posterior PDF of each lithology type that were produced from six inversion tests is shown in Figures 4.27 to 4.32. Overall, P-impedance shows a better match between prior and posterior PDF, while Vp/Vs and density provided poor distribution of posterior PDF. This might be caused by the short streamer length used during seismic acquisition. The 3D seismic data therefore did not contain sufficient far-angle data to derive reliable Vp/Vs and density estimates. Moreover, the posterior PDF of H30 generally showed a better match with the prior PDF than the results obtained from the deeper reservoir in H37, and might relate to the reduced seismic data quality with increasing time/depth.

Analysis of all the QC results showed that Test 18 provided the best result in terms of posterior proportion, posterior PDF, and distribution of each lithology type, also when compared to the lithology log at the well locations. Based on this it was decided to use the inversion parameters of Test 18 in the final inversions.

Table 4.3 Summary of inversion parameter settings for variogram, PDF, input gather, and seismic S/N ratio test.

Test No.	Variogram Range (ms, m)			S/N				Prior (H30)		Prior (H37)		Key Parameters Change	Wells Condition	Comments
	Shale	Sand	Coal	Near	Near-Mid	Mid	Far	Sand (%)	Coal (%)	Sand (%)	Coal (%)			
1	6, 600	6, 600	1, 1500	10	10	10	10	11	1	9	1	Long vriogram range	Blind	Overestimate posterior %sand and %coal
2	**6, 601**	**6, 600**	**1, 1500**	**10**	**10**	**10**	**10**	**11**	**1**	**9**	**1**	**Long vriogram range**	**Constrain**	**Overestimate posterior %sand and %coal**
3	4, 400	3, 300	1, 1500	10	10	10	10	11	1	9	1	Short vriogram range	Blind	Better posterior proportion, Bad posterior PDF
4	4, 400	3, 300	1, 1500	10	10	10	10	11	1	9	1	Modify PDF	Blind	Better posterior proportion, Good posterior PDF
5	**4, 400**	**3, 300**	**1, 1500**	**10**	**10**	**10**	**10**	**11**	**1**	**9**	**1**	**Modify PDF**	**Constrain**	**Better posterior proportion, Good posterior PDF**
6	4, 400	3, 300	1, 1500	10	10	10	10	11	1	9	1	Modify PDF	Blind	Better posterior proportion, BUT bad posterior PDF
7	4, 400	3, 300	1, 1500	7	10	10	5	11	1	9	1	S/N (SN1)	Blind	Better litholofacies section (match to wells)
8	4, 400	3, 300	1, 1500	7	12	12	5	11	1	9	1	S/N (SN2)	Blind	SN1 and SN2 show similar posterior PDF
9	**4, 400**	**3, 300**	**1, 1500**	**7**	**10**	**10**	**5**	**11**	**1**	**9**	**1**	**S/N (SN1)**	**Constrain**	**Match with well, BUT some gas sand become coal in H30 layer**
10	4, 400	3, 300	1, 1500	7	10	10	5	11	1	9	1	Adjust coal PDF	Blind	Good Posterior PDF, Gas sand = coal in H30 layer
11	4, 400	3, 300	1, 1500	7	10	10	5	7	1	5	1	Decrease prior sand percentage	Blind	Good Posterior PDF, decrease posterior %sand
12	**4, 400**	**3, 300**	**1, 1500**	**7**	**10**	**10**	**5**	**7**	**1**	**5**	**1**	**Decrease prior sand percentage**	**Constrain**	**Good Posterior PDF, decrease posterior %sand, match to wells**
13	4, 400	3, 300	1, 1500	7	10	10	5	11	1	9	1	Adjust coal PDF (higher Vp/Vs)	Blind	Bad posterior PDF of Shale in H30 layer
14	4, 400	3, 300	1, 1500	7	10	10	5	11	1	9	1	Adjust shale PDF	Blind	Good posterior PDF, BUT increase posterior sand proportion
15	4, 400	3, 300	1, 1500	7	10	10	5	6	1	4	1	Decrease prior sand percentage	Blind	Thick sand in H30 match to well, BUT posterior %sand is still high especially H37
16	**4, 400**	**3, 300**	**1, 1500**	**7**	**10**	**10**	**5**	**6**	**1**	**4**	**1**	**Decrease prior sand percentage**	**Constrain**	**Thick sand in H30 match to well, BUT posterior %sand is still high especially H37**
17	4, 400	3, 300	1, 1500	7	10	10	5	7	1	5	1	Adjust sand PDF (more separate from Shale)	Blind	Good Posterior PDF, decrease posterior %sand, match to wells
18	**4, 400**	**3, 300**	**1, 1500**	**7**	**10**	**10**	**5**	**7**	**1**	**5**	**1**	**Adjust sand PDF (more separate from Shale)**	**Constrain**	**Good Posterior PDF, decrease posterior %sand and %coal, match to wells**

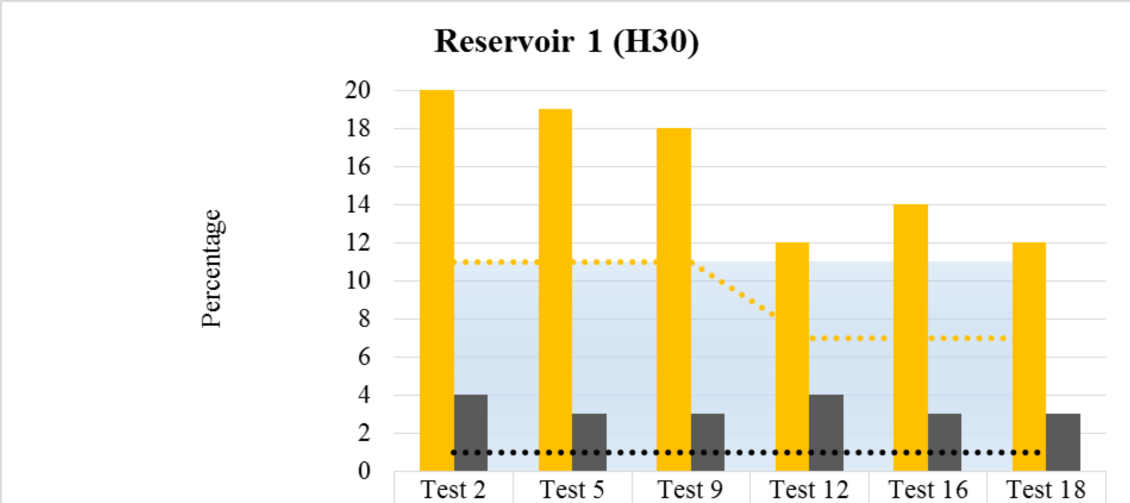

	Test 2	Test 5	Test 9	Test 12	Test 16	Test 18
Sand (from input wells)	11	11	11	11	11	11
Posterior (Sand)	20	19	18	12	14	12
Posterior (Coal)	4	3	3	4	3	3
Prior (Sand)	11	11	11	7	7	7
Prior (Coal)	1	1	1	1	1	1

Figure 4.19 Comparison of prior and posterior proportions of each lithology in Reservoir 1.

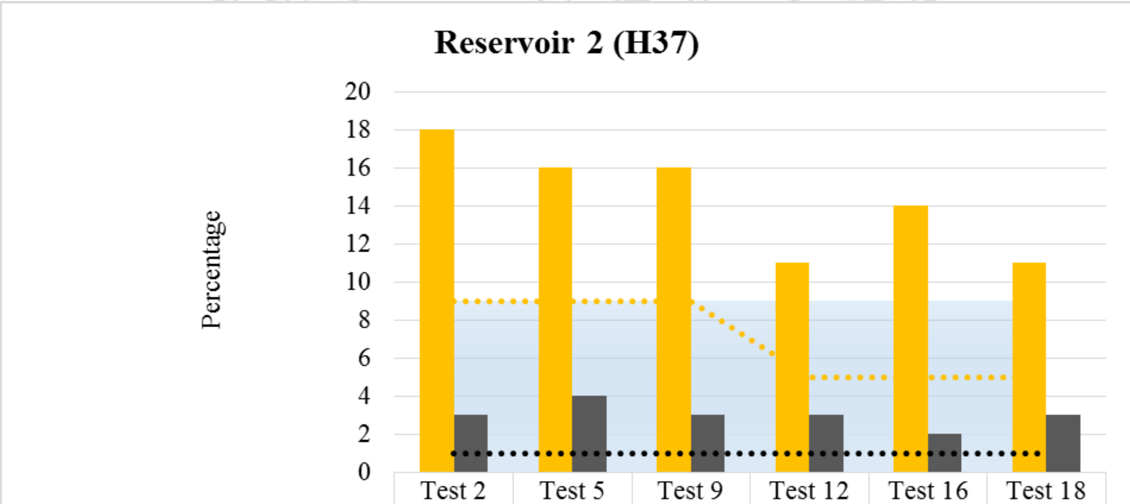

	Test 2	Test 5	Test 9	Test 12	Test 16	Test 18
Sand (from input wells)	9	9	9	9	9	9
Posterior (Sand)	18	16	16	11	14	11
Posterior (Coal)	3	4	3	3	2	3
Prior (Sand)	9	9	9	5	5	5
Prior (Coal)	1	1	1	1	1	1

Figure 4.20 Comparison of prior and posterior proportions of each lithology in Reservoir 2.

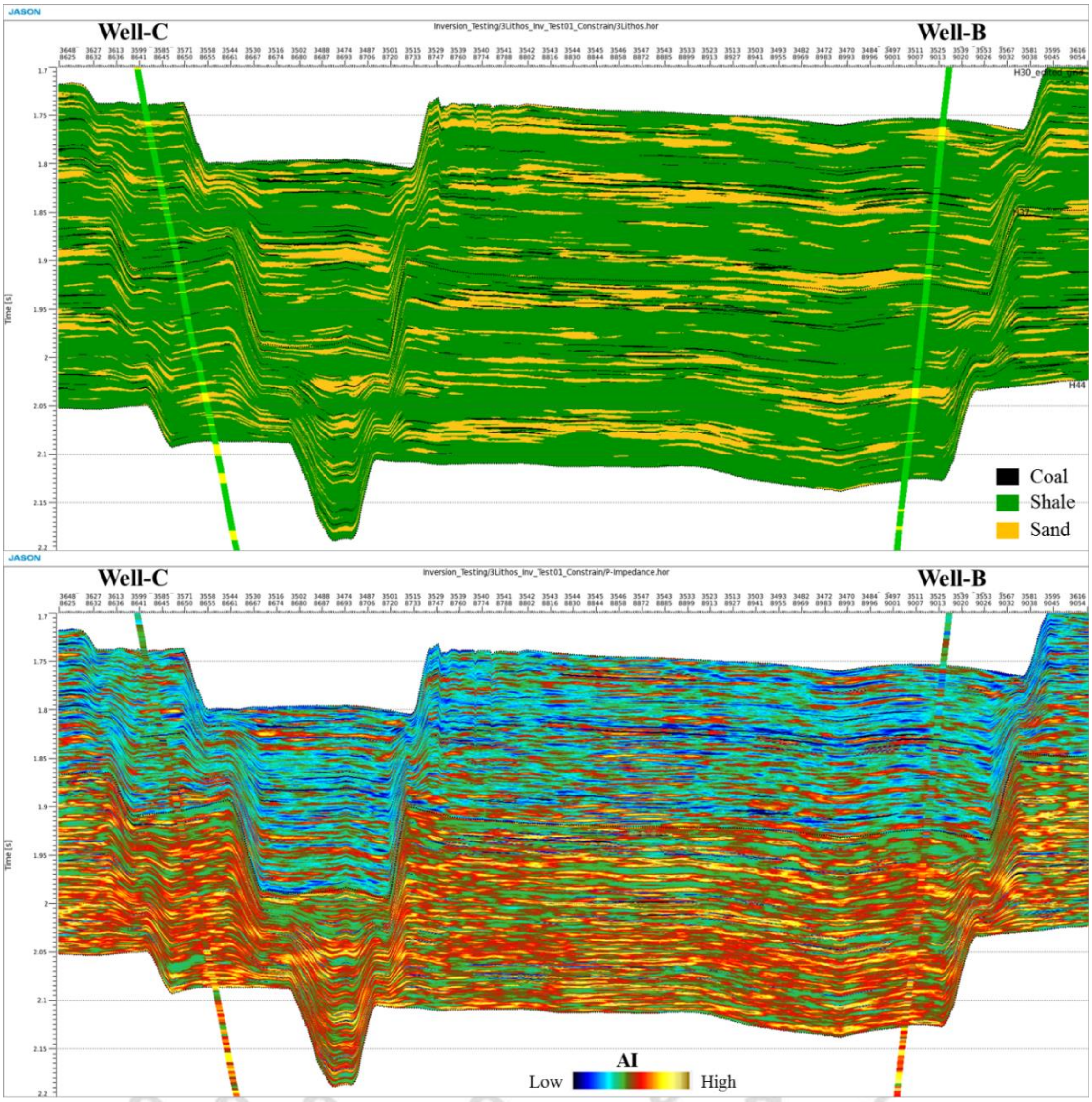

Figure 4.21 Arbitrary sections of lithofacies (above) and P-impedance (below) generated from inversion Test 2 (long-range variogram).

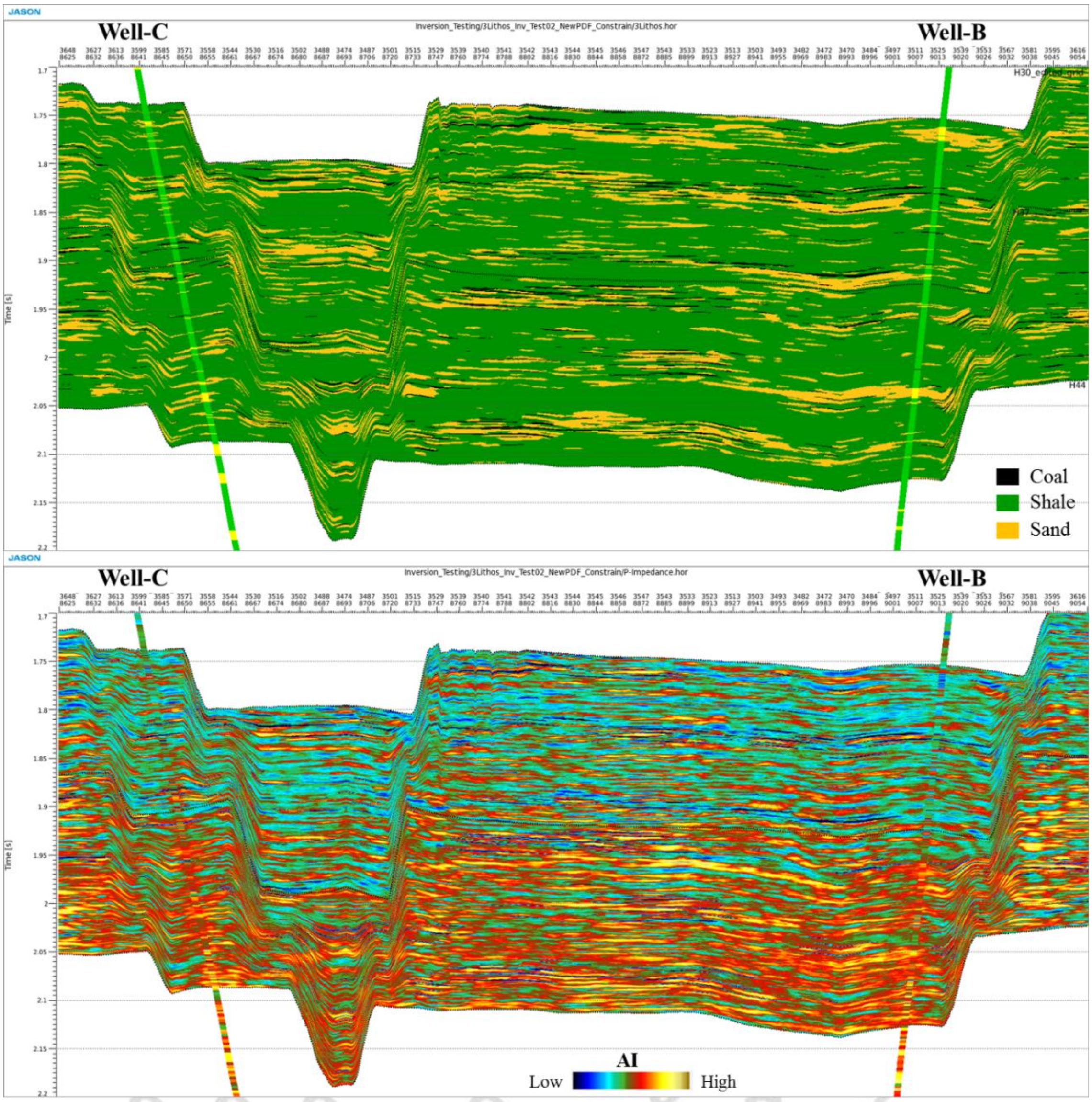

Figure 4.22 Arbitrary sections of lithofacies (above) and P-impedance (below) generated from inversion Test 5 (short-range variogram).

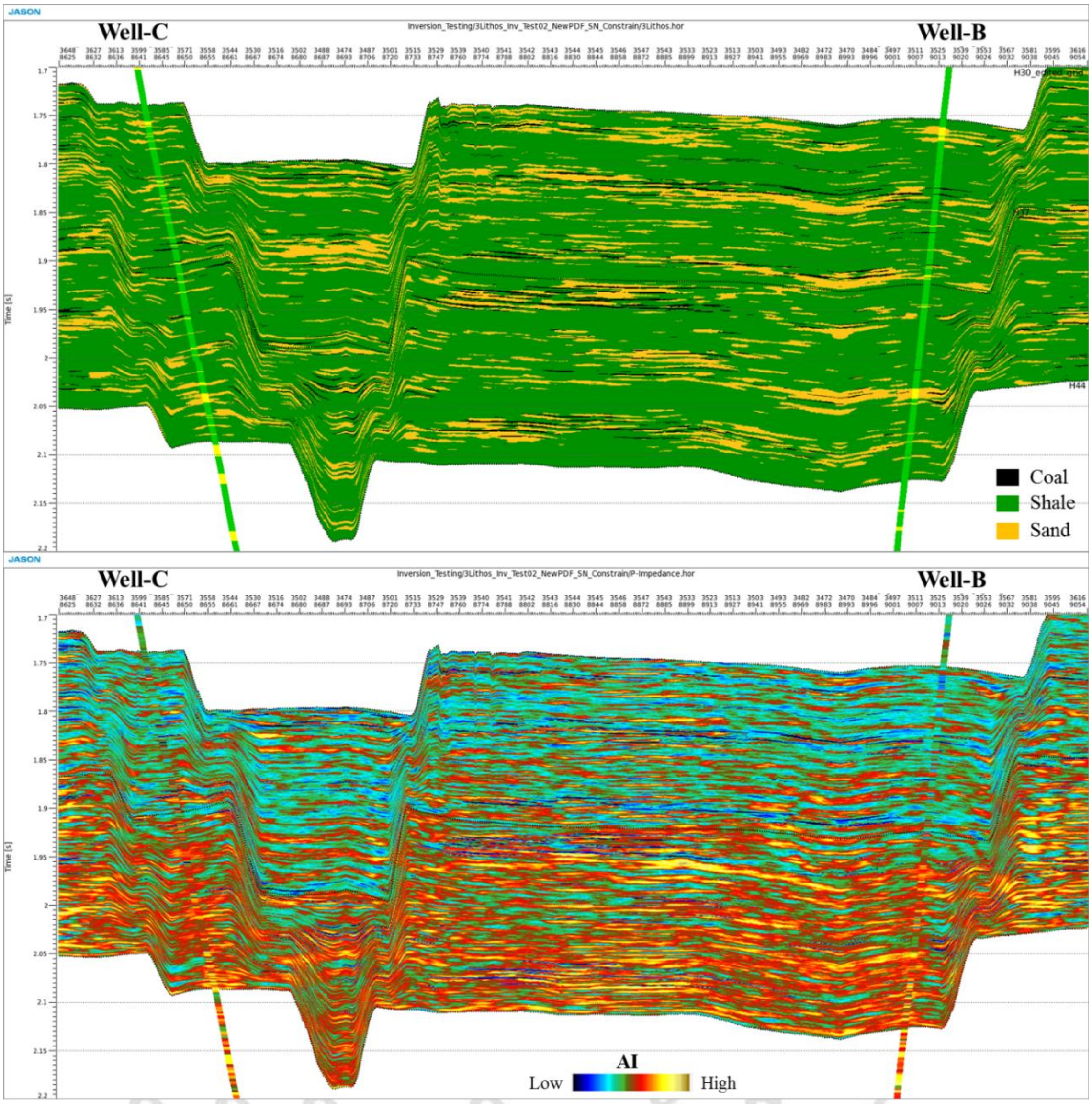

Figure 4.23 Arbitrary sections of lithofacies (above) and P-impedance (below) generated from inversion Test 9 (decreased S/N).

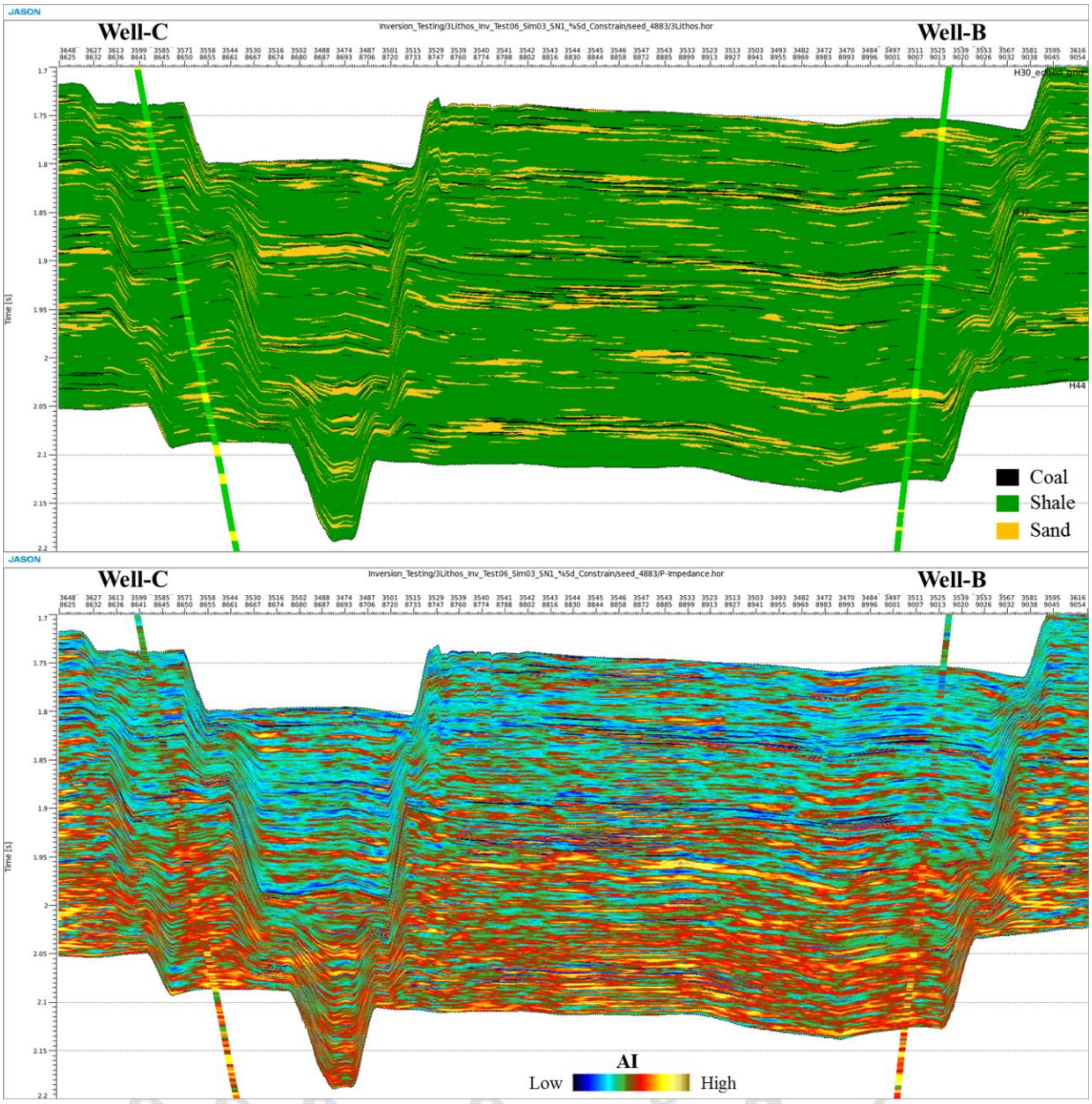

Figure 4.24 Arbitrary sections of lithofacies (above) and P-impedance (below) generated from inversion Test 12 (decreased prior sand proportion).

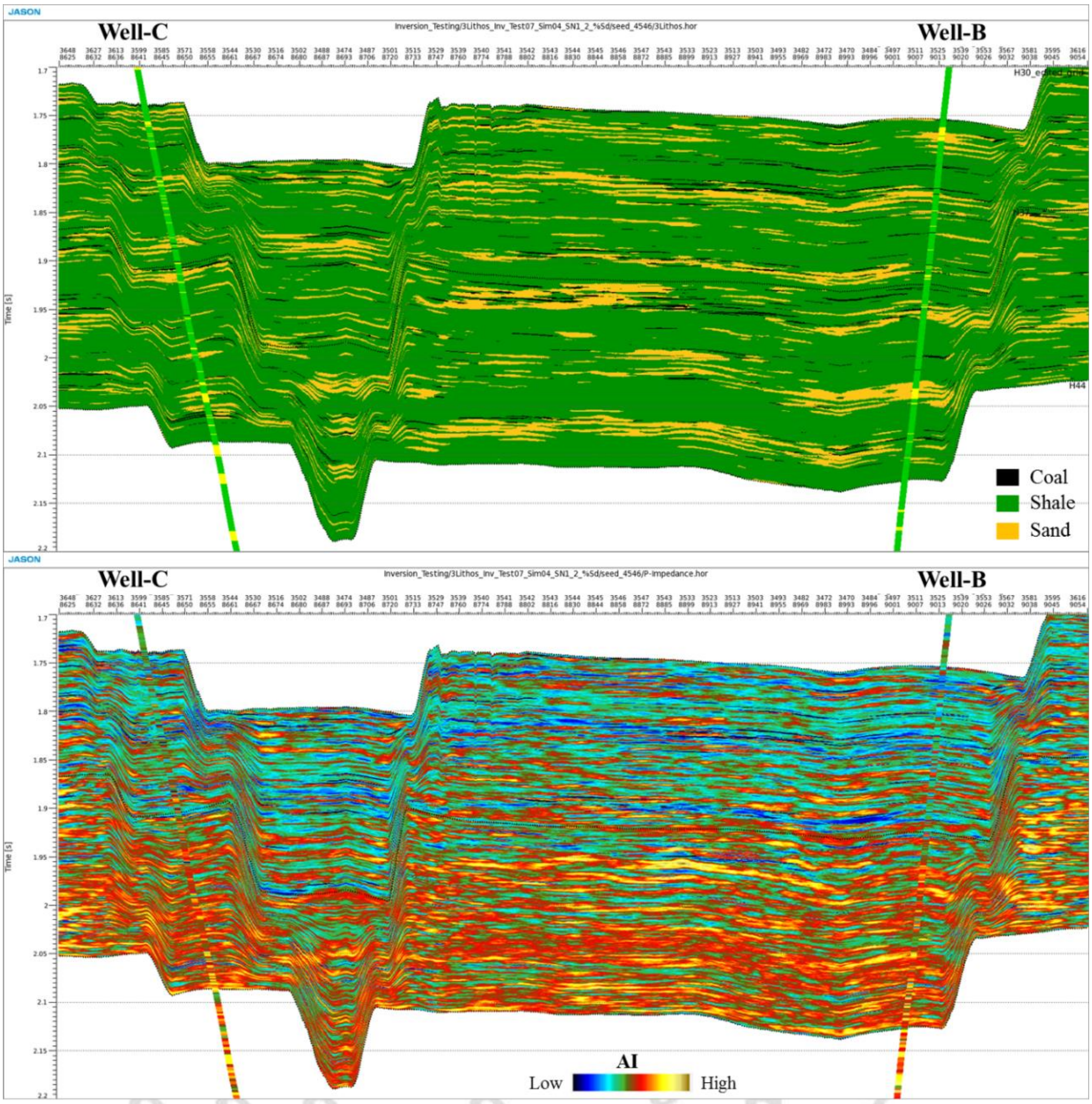

Figure 4.25 Arbitrary sections of lithofacies (above) and P-impedance (below) generated from inversion Test 16 (modified prior coal PDF).

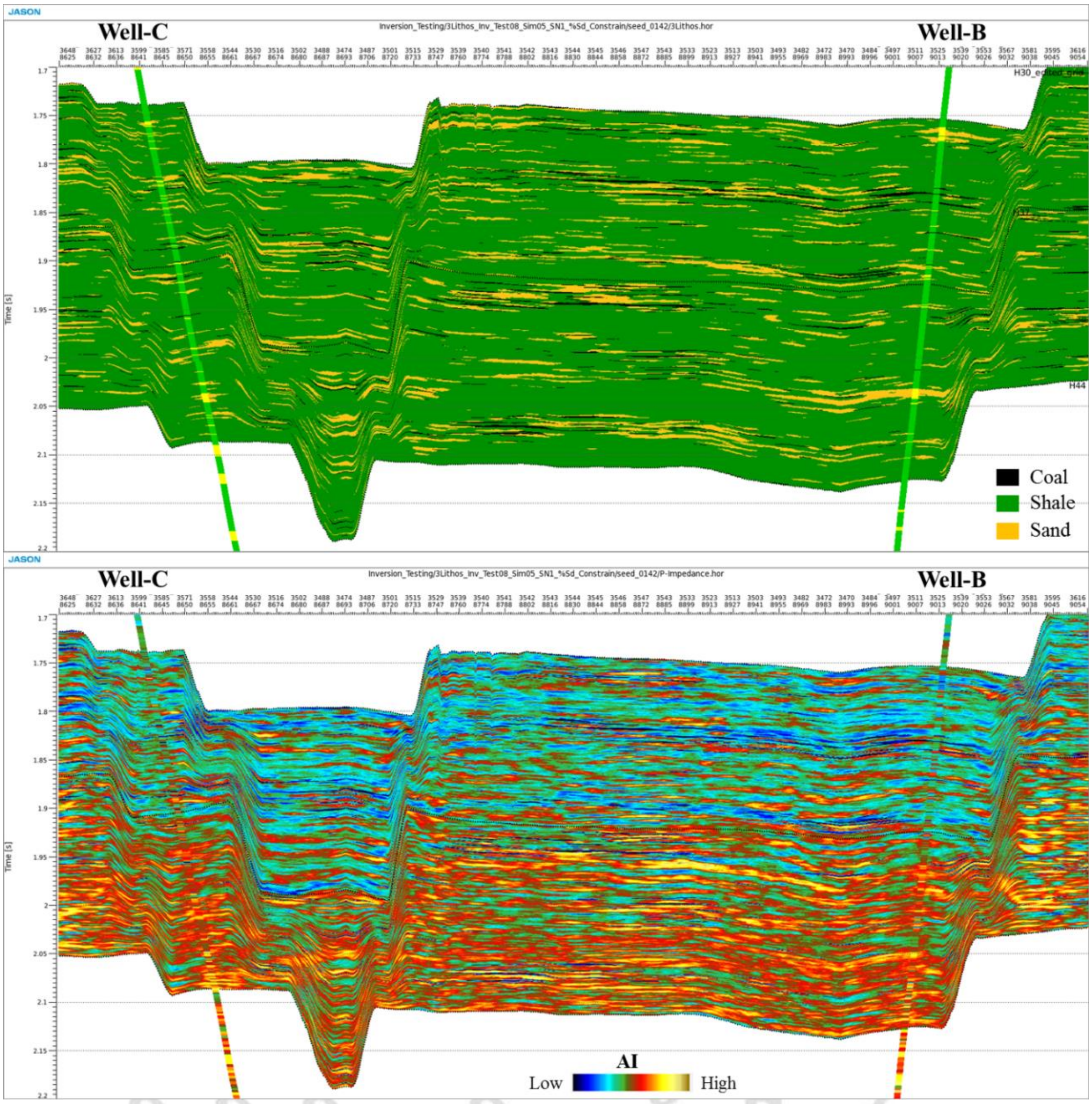

Figure 4.26 Arbitrary sections of lithofacies (above) and P-impedance (below) generated from inversion Test 18 (modified prior sand PDF).

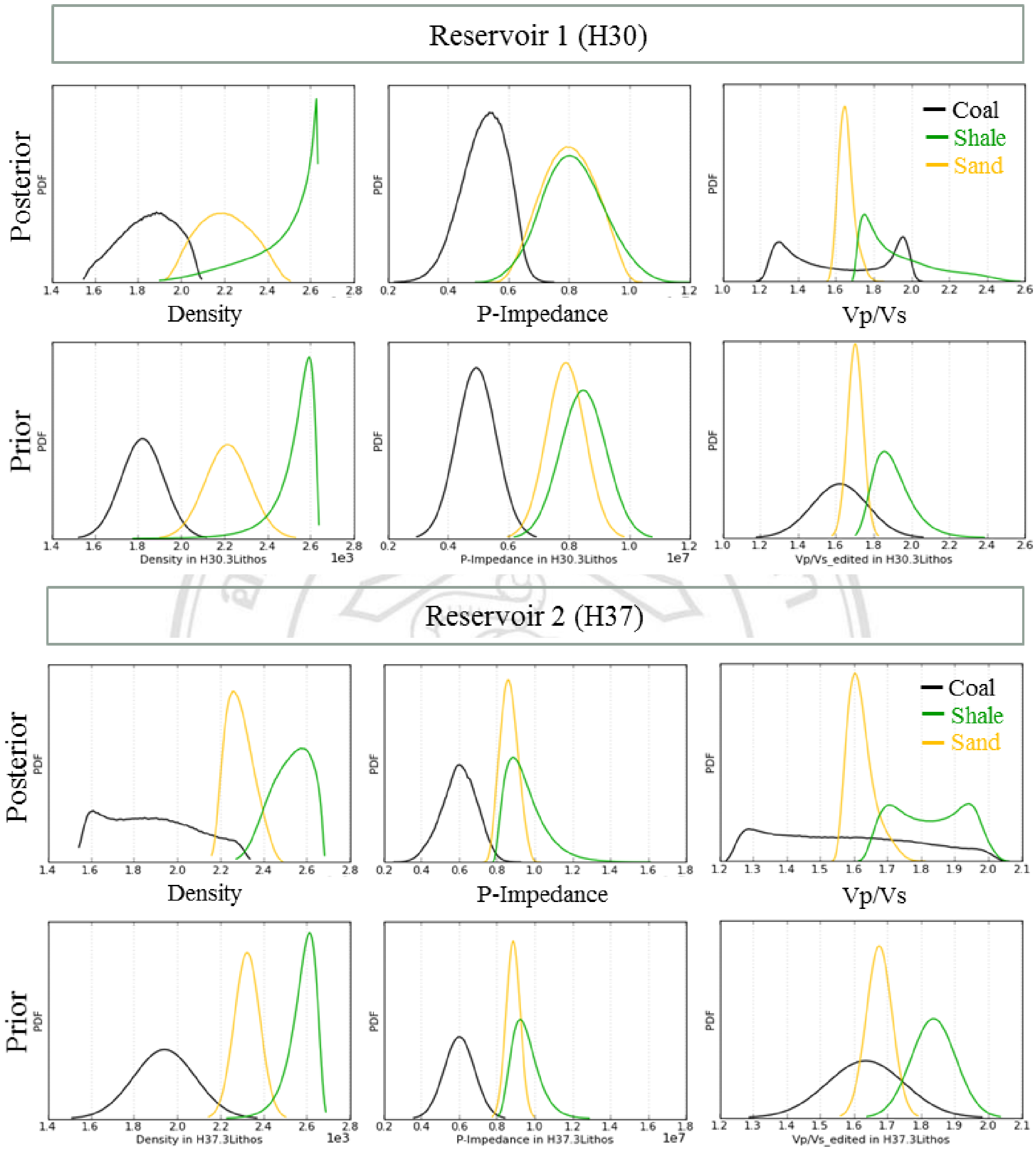

Figure 4.27 Comparison of prior and posterior PDF of each lithology type generated from inversion Test 2 (long-range variogram).

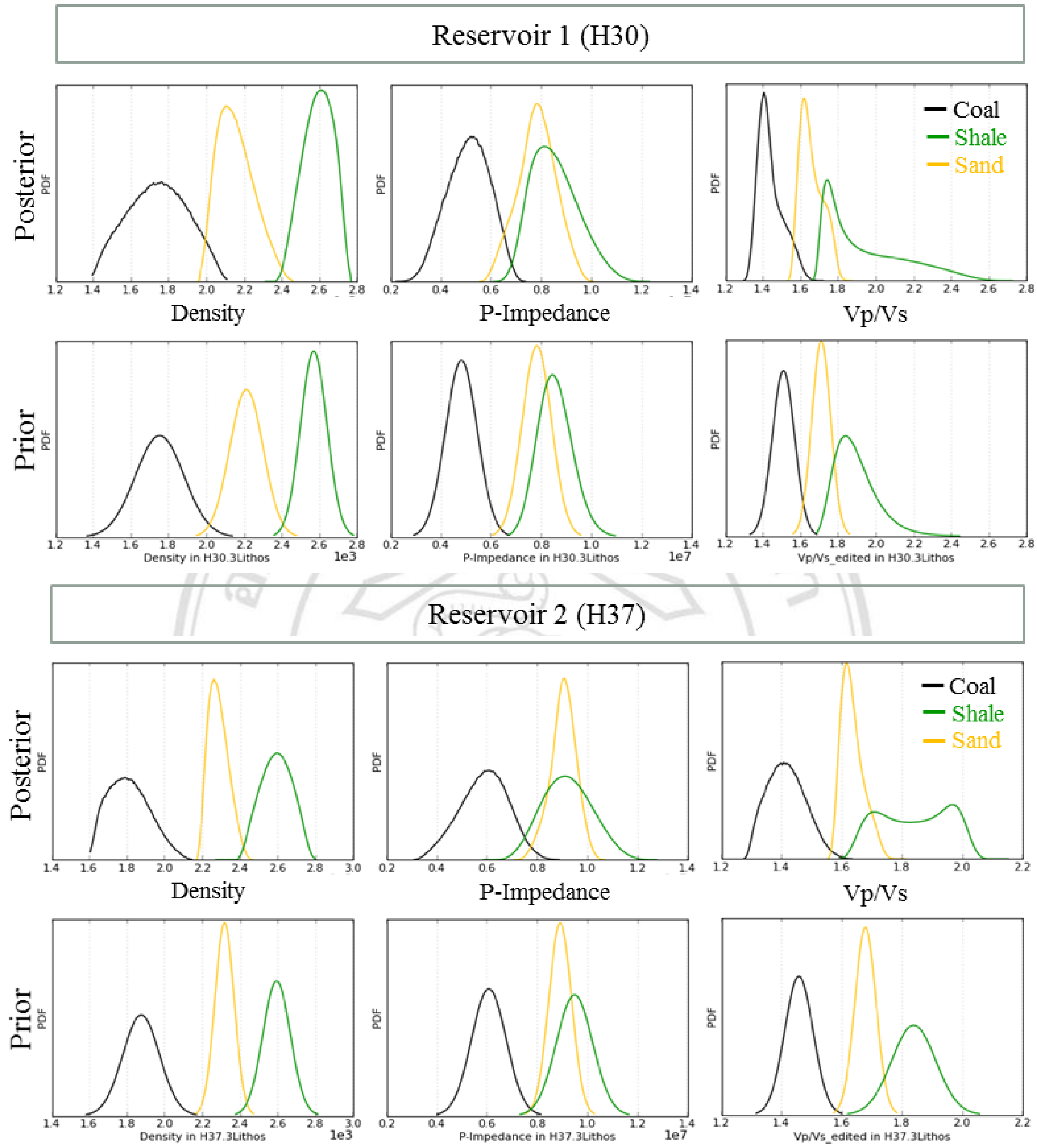

Figure 4.28 Comparison of prior and posterior PDF of each lithology type generated from inversion Test 5 (short-range variogram).

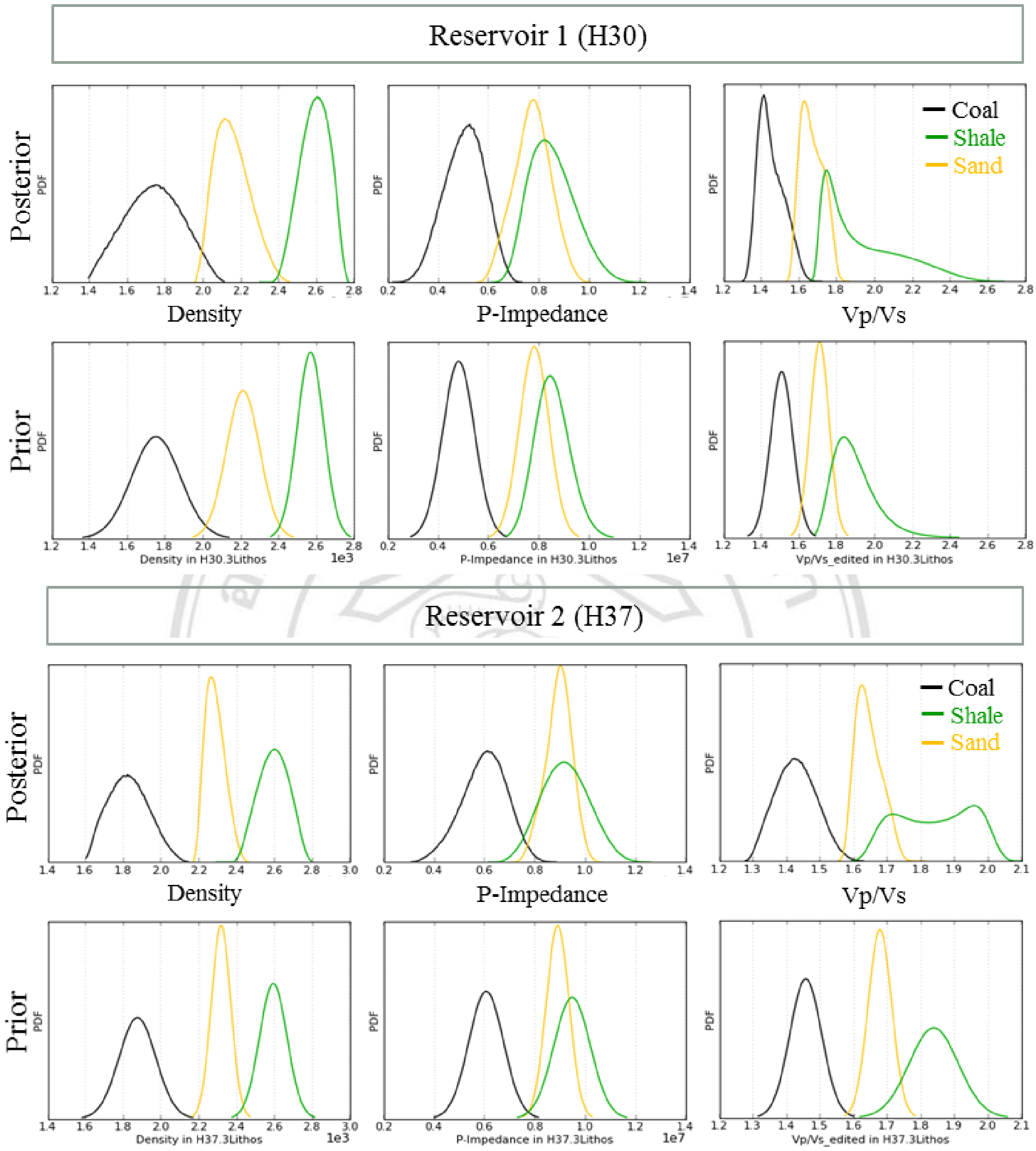

Figure 4.29 Comparison of prior and posterior PDF of each lithology type generated from inversion Test 9 (decreased S/N).

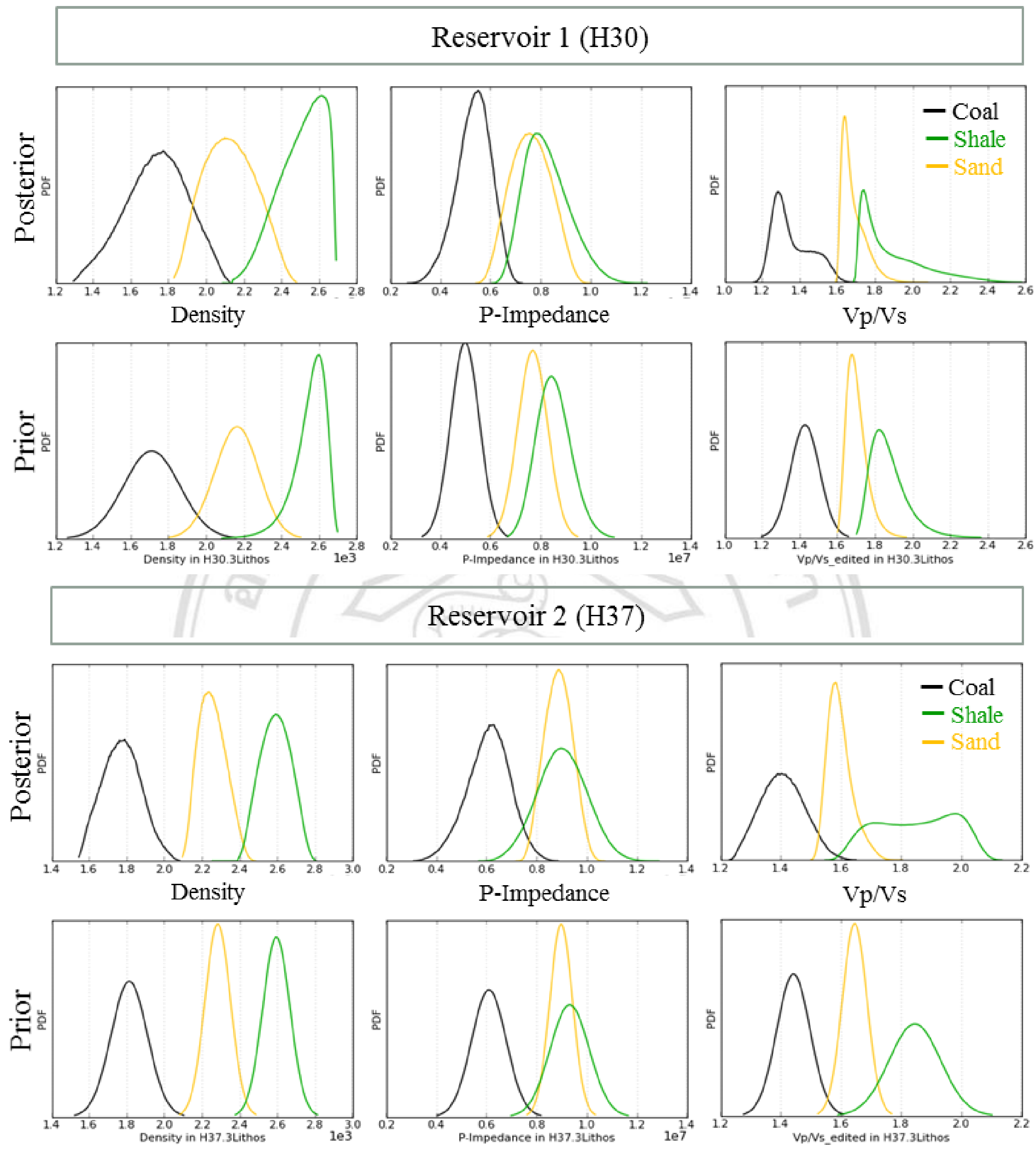

Figure 4.30 Comparison of prior and posterior PDF of each lithology type generated from inversion Test 12 (decreased prior sand proportion).

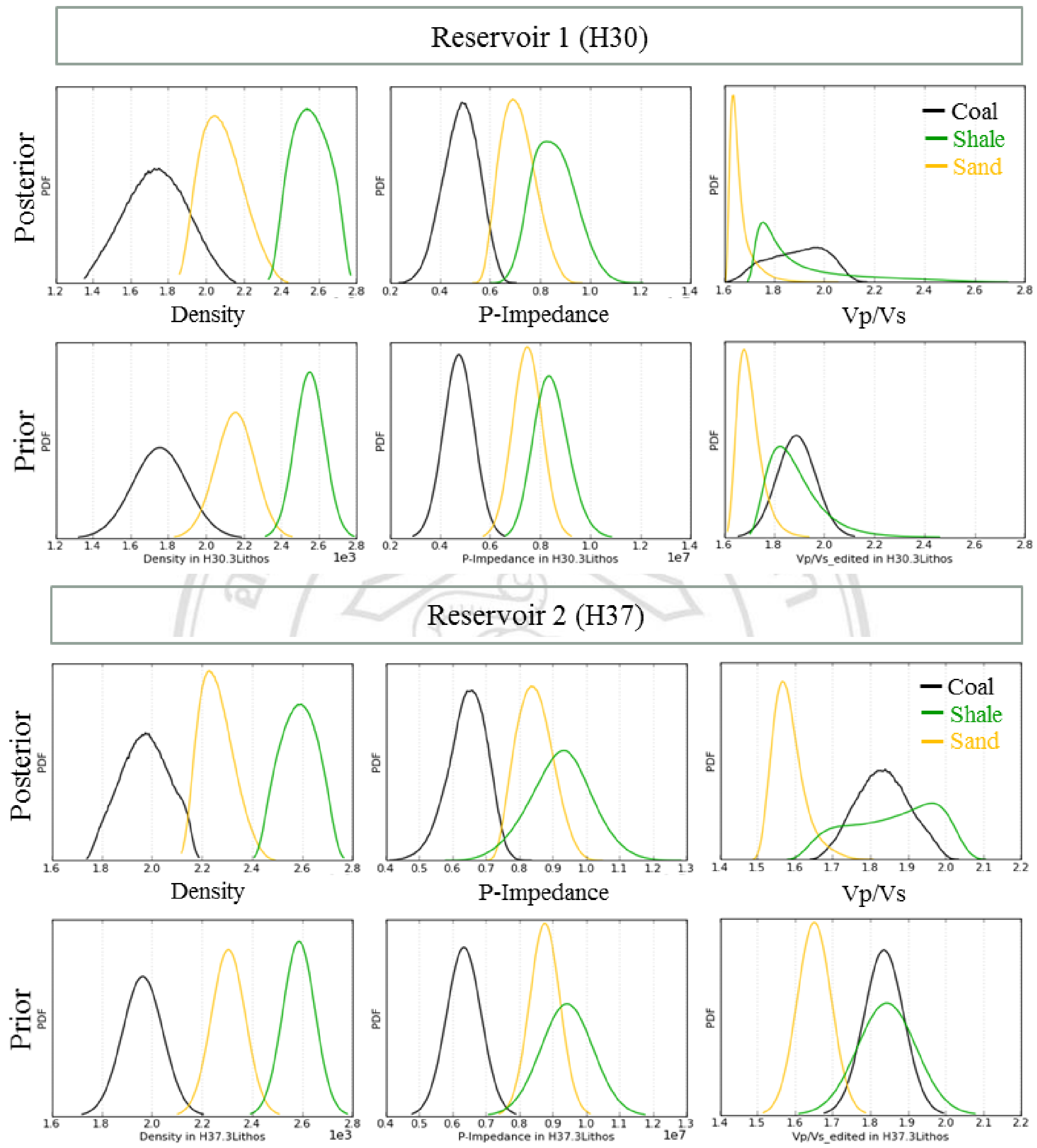

Figure 4.31 Comparison of prior and posterior PDF of each lithology type generated from inversion Test 16 (modified prior coal PDF).

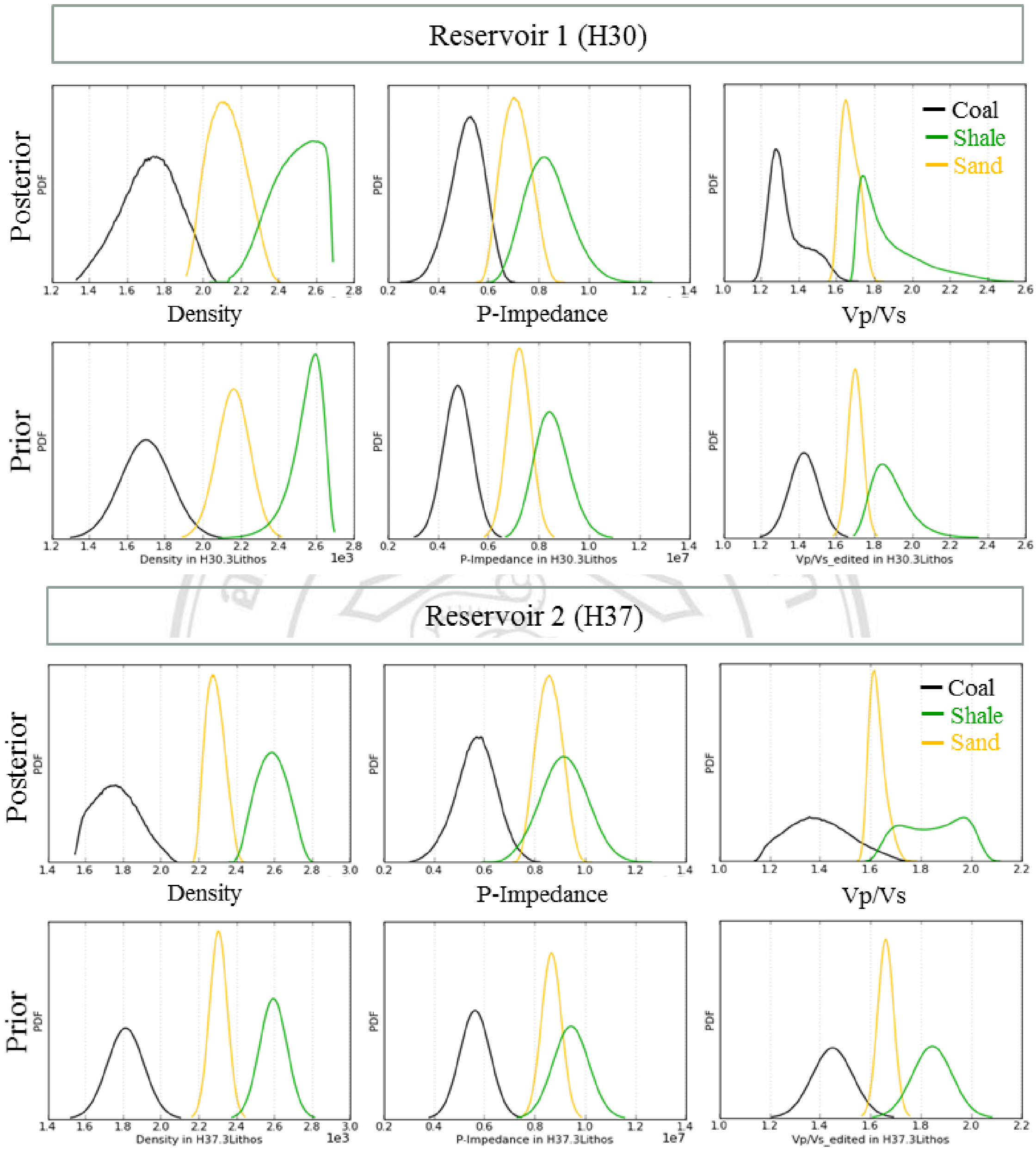

Figure 4.32 Comparison of prior and posterior PDF of each lithology type generated from inversion Test 18 (modified prior sand PDF).

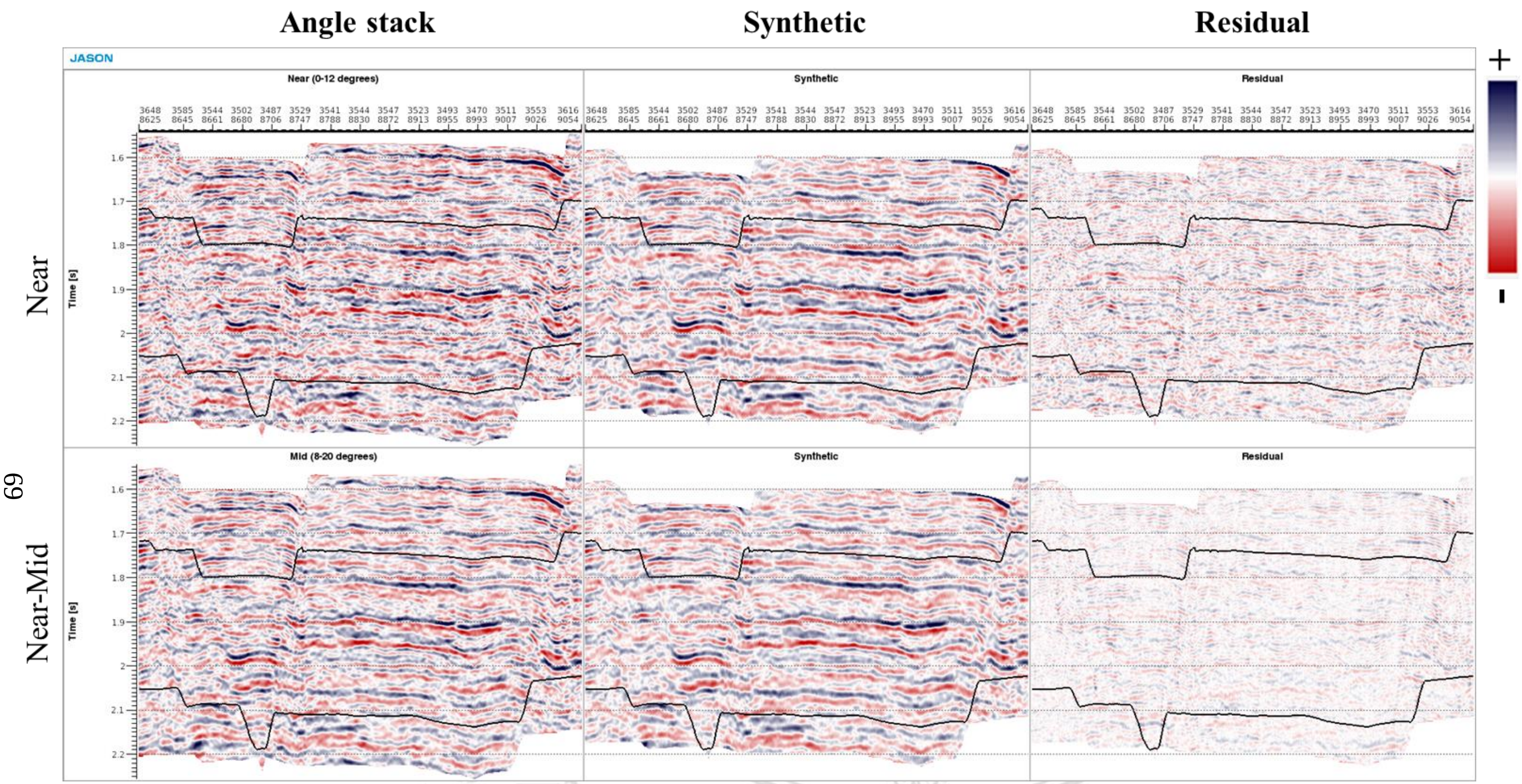

Figure 4.33 Synthetic and residual sections of near and near-mid angle stack generated from inversion Test 18.

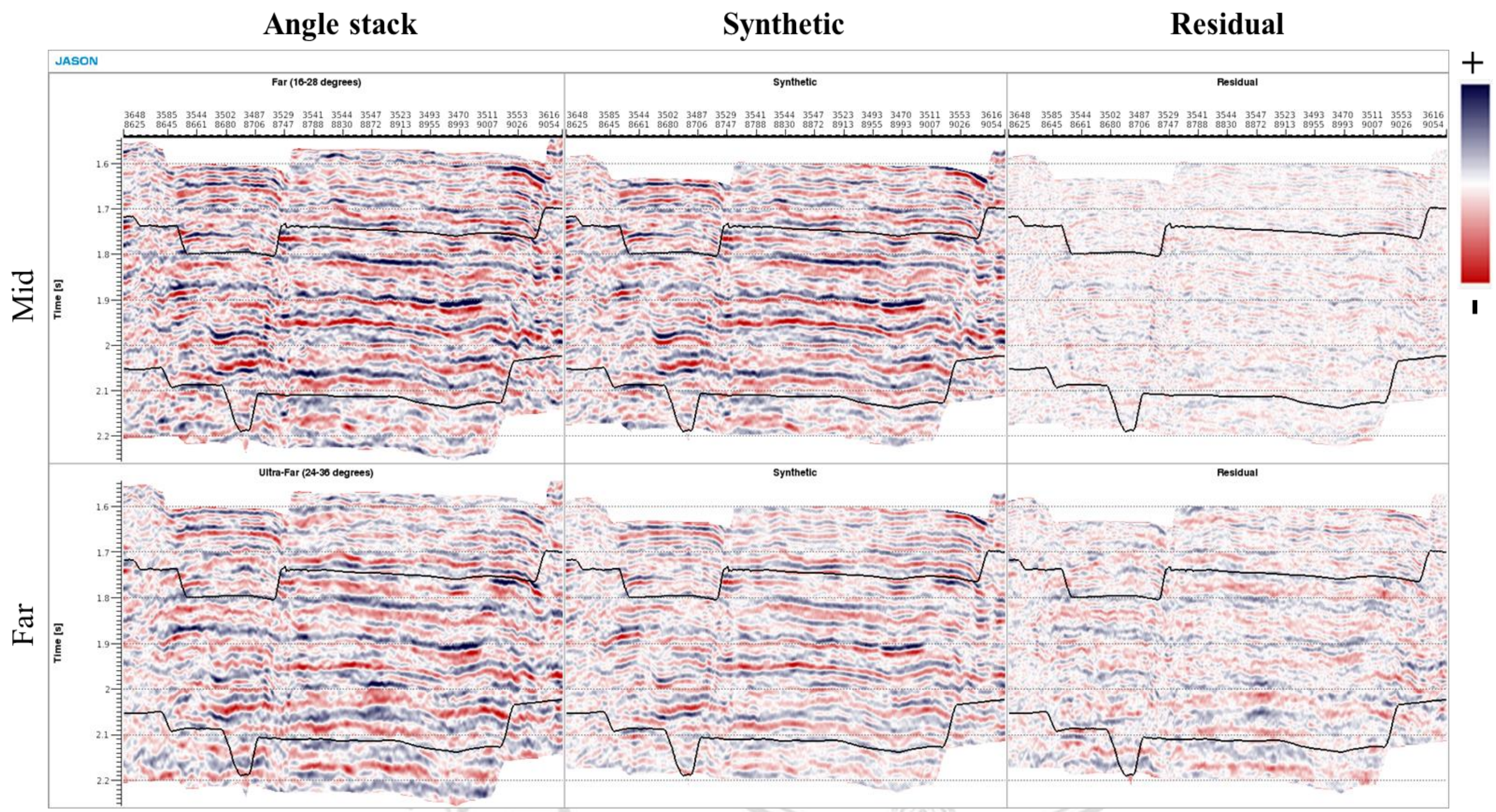

Figure 4.34 Synthetic and residual sections of mid and far angle stack generated from inversion Test 18.